RSC Advances

REVIEW

View Article Online
View Journal | View Issue

Cite this: *RSC Adv.*, 2019, **9**, 41684

A walk around the application of nanocatalysts for cross-dehydrogenative coupling of C–H bonds

Jianjie Wang,[a] Pingyang Su,[b] Shahrzad Abdolmohammadi*[c] and Esmail Vessally[d]

Cross-dehydrogenative coupling reactions between two unmodified C–H bonds are one of the most attractive and fundamental strategies for the construction of C–C bonds. As these reactions avoid pre-functionalization and de-functionalization of the substrates, they are cleaner, safer, and faster than traditional cross-coupling reactions. After the introduction of the modern area of cross-dehydrogenative coupling in 2003, many efforts have been devoted to the development of more efficient and selective catalytic systems for these appealing reactions. Among the different types of catalytic systems that have been investigated, nanostructured metal catalysts are highly attractive in view of their high catalytic performance, easy separability and good reusability. The purpose of this review is to focus on the application of nanocatalysts for cross-dehydrogenative coupling of C–H bonds with particular emphasis on the mechanistic aspects of the reactions. Specifically, we have structured this review based on the type of C–C bonds. Thus, the review is divided into six major sections: (i) C(sp^3)–C(sp^3) coupling; (ii) C(sp^3)–C(sp^2) coupling; (iii) C(sp^3)–C(sp) coupling; (iv) C(sp^2)–C(sp^2) coupling; (v) C(sp^2)–C(sp) coupling; and (vi) C(sp)–C(sp) coupling.

Received 24th October 2019
Accepted 28th November 2019

DOI: 10.1039/c9ra08752d

rsc.li/rsc-advances

1. Introduction

Carbon–carbon (C–C) bond formation represents a key step in the synthesis of organic materials and provides the foundation for constructing more complicated organic molecules from the simpler ones.[1] The use of transition-metal-catalyzed cross-coupling reactions for the fabrication of C–C bonds has increased tremendously over the past few decades.[2] Among the

[a]*College of Applied Mathematics, Shanxi University of Finance and Economics, Taiyuan, Shanxi 030006, China*

[b]*College of Chemistry and Molecular Engineering, Shanghai 200240, China*

[c]*Department of Chemistry, East Tehran Branch, Islamic Azad University, P. O. Box 18735-138, Tehran, Iran. E-mail: s.abdolmohamadi@iauet.ac.ir; s.abdolmohamadi@yahoo.com*

[d]*Department of Chemistry, Payame Noor University, Tehran, Iran*

Shahrzad Abdolmohammadi was born in Iran, in 1976. She received her BSc degree in chemistry from Alzahra University (AU), Tehran, Iran, in 1999, her MSc degree in organic chemistry from the Tarbiat_Modarres University (TMU), Tehran, Iran under the supervision of Professor Issa Yavari in 2002 and her PhD degree in organic chemistry from the Tehran University (TU), Tehran, Iran, under the supervision of Professor Hooshang Pirelahi and Professor Saeed Balalaie, in 2008. She is associate professor in East Tehran Branch, Islamic Azad University, Tehran, Iran. Her research interests include organic synthesis, heterocyclic synthesis, multicomponent reactions, nanocatalysis, organocatalysis, and synthetic methodology.

Esmail Vessally was born in Sharabiyan, Sarab, Iran, in 1973. He received his BS degree in pure chemistry from university of Tabriz, Tabriz, Iran, and his MS degree in organic chemistry from Tehran university, Tehran, Iran, in 1999 under the supervision of Prof. H. Pirelahi. He completed his PhD degree in 2005 under the supervision of Prof. M. Z. Kassaee. Now he is working at Payame Noor University as Professor in organic chemistry. His research interests include theoretical organic chemistry, new methodologies in organic synthesis and spectral studies of organic compounds.

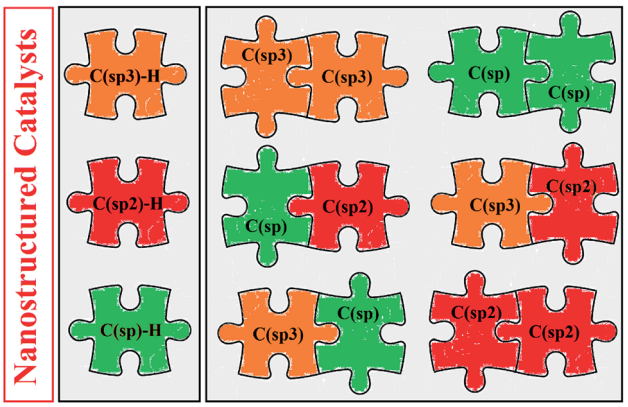

Fig. 1 Nanoparticles catalyzed cross-dehydrogenative coupling of C–H bonds.

various C–C cross-coupling reactions, Suzuki, Sonogashira, Heck, Hiyama, Stille, Negishi, and Kumada–Corriu reactions find maximum application not only in academic laboratories but also in industrial processes.[3] However, these reactions require at least one pre-functionalized partner to generate the desired products and therefore suffer from non-availability of starting materials and/or hazardous waste streams. Cross-dehydrogenative coupling reactions between two unmodified C–H bonds are the most atom-economical and sustainable synthetic alternatives to traditional coupling procedures since they avoid pre-functionalization and de-functionalization of the substrates and formally they loss non-toxic H_2 as only by-product.[4] In view of the high importance of this branch of cross-coupling reactions, many researchers have been working to explore novel and more efficient catalytic systems that can operate at lower loading and temperatures.

Over the past few years, nanoparticles (NPs) have gained much attention in both organic and inorganic synthesis as easily separable, reusable and environmentally sustainable catalysts.[5] The high surface area per unit mass and reactive morphology of nanoparticles made them very successful heterogeneous catalysts in various organic transformations.[5,6] In this context, a number of nanostructured catalytic systems have been developed in recent years which effectively promoted cross-dehydrogenative coupling reactions. To the best of our knowledge, a comprehensive review has not appeared on the application of nanocatalysts for cross-dehydrogenative coupling of C–H bonds in the literature thus far. In continuation of our preceding reviews on cross-coupling reactions, heterocyclic synthesis[7] and application of nanocatalysts in organic synthesis,[5b,c,6] in this review, we will highlight the most representative reports on the C–C bond forming reactions through nanoparticles catalyzed cross-dehydrogenative coupling of C–H bonds until September 2019 (Fig. 1), by hoping that it will be beneficial to the development of novel and truly efficient catalytic systems for this hot and fast growing research topic.

2. Constructing C(sp^3)–C(sp^3) bonds

Transition-metal-catalyzed oxidative cross-coupling of two C(sp^3)–H bonds has emerged as the most attractive and also the most challenging strategy for the construction of C(alkyl)–C(alkyl) bonds.[8] The difficulty arises due to their sluggish transmetalation and thus the reactive organometallic intermediates are susceptible to side reactions.[9] Therefore, many researchers have been working to explore the more effective catalytic systems for this appealing synthetic strategy. In this context, several nanostructured catalysts have been developed and successfully utilized.

In 2010, Song and Li along with their co-workers studied the oxidative aza-Henry reactions using magnetite nanoparticles (Fe_3O_4 NPs) as the catalyst.[10] Hence, a variety of β-nitroamine derivatives **3** were smoothly obtained in moderate to excellent yields through the reaction of corresponding *N*-aryl-1,2,3,4-tetrahydroisoquinolines **1** with nitroalkanes **2** *via* oxidative functionalization of α-C(sp^3)–H bonds adjacent to nitrogen atoms (Scheme 1). However, 1-phenylpyrrolidine did not work well in the reaction and therefore no other pyrrolidines were examined in the protocol. Noteworthy, nitroalkanes playing a dual role in this coupling reaction; the substrate and the solvent. Extension to oxidative Mannich reaction between tetrahydroisoquinolines and acetone were attempted and the corresponding coupling products were isolated in moderate yields. It is notable that the nanocatalyst can be easily separated from the final reaction mixture by means of an external magnet, washing with ethyl acetate, and air-dried, and then be reused for at least nine times with tangible decrease in its catalytic activity. The authors proposed reaction mechanism for this oxidative coupling reaction is illustrated in Scheme 2. The reaction starts with the oxidation of tertiary amine **1** by O_2 in the presence of Fe_3O_4 nanoparticles, leading to the generation of the iminium cation **A**. Meanwhile, deprotonation of nitroalkane **2** under the reaction condition leads to intermediate **B**. Finally, coupling of

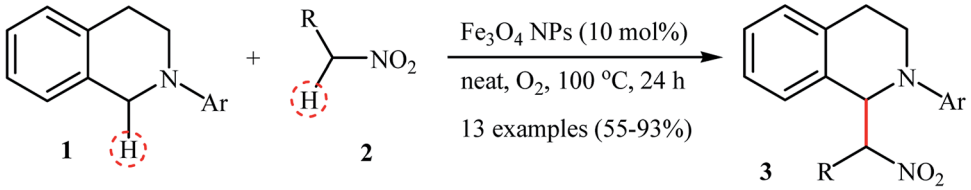

Ar= Ph, 4-C_6H_4, 4-OMe-C_6H_4, 4-Br-C_6H_4, 3-OMe-C_6H_4, 2-OMe-C_6H_4
R= H, Me, Et

Scheme 1 Fe_3O_4 NPs-catalyzed oxidative aza-Henry reaction.[10]

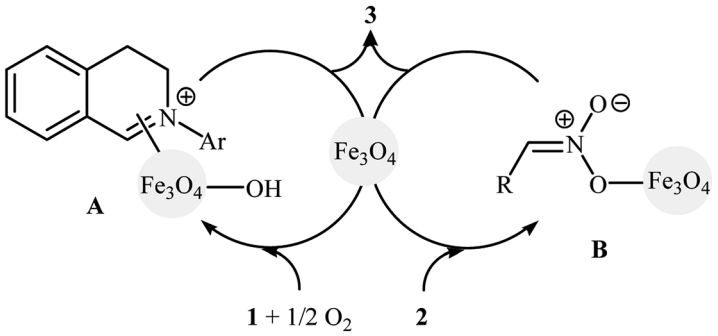

Scheme 2 Proposed mechanism for the Fe_3O_4 NPs-catalyzed cross-dehydrogenative coupling of tertiary amines **1** with nitroalkanes **2**.[10]

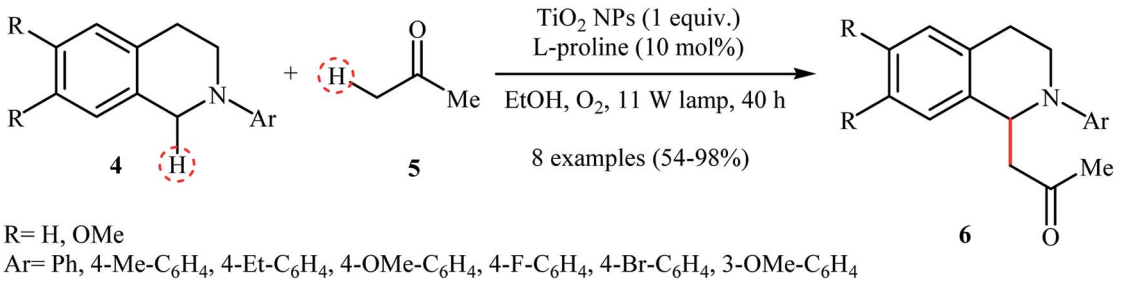

Scheme 3 Rueping's synthesis of amino-ketones **6**.[11]

the two intermediates **A** and **B** affords the desired product **3** and regenerates the Fe_3O_4 nanoparticles.

A similar example of the oxidative aza-Henry reaction by a nanocatalyst was disclosed by Rueping and co-workers in 2012, when they reported about the use of commercially available TiO_2 nanoparticles (Evonik-Degussa Aeroxide P25) to promote the oxidative coupling of a series of *N*-aryl-1,2,3,4-tetrahydroisoquinolines with nitromethane in EtOH under irradiation of visible light.[11] The catalytic system was also effective for the oxidative Mannich reaction of tetrahydroisoquinoline derivatives **4** with acetone **5** to provide the target amino-ketones **6** in moderate to almost quantitative yields (Scheme 3).

Concurrently, Wu's research team showed that graphene-supported RuO_2 nanoparticles (G-RuO_2 NPs) were able to promote the aza-Henry reaction of 2-aryl-substituted tetrahydroisoquinolines with nitroalkanes in the absence of any ligand or additive in the most environmentally benign solvent, water.[12] Significantly, the nanocomposite has been made *in situ* from water-soluble sulfonic-group-functionalized graphene and $RuCl_3$ hydrate. The nanocomposite has been characterized by using various analyses such as transmission electron microscopy (TEM), energy-dispersive spectroscopy (EDS) and X-ray photoelectron spectroscopy (XPS). The size of nanoparticles was found to be about 2 nm by TEM technique. A comparison of the catalytic performance of the G-RuO_2 NPs, $RuCl_3 \cdot nH_2O$ and $RuO_2 \cdot nH_2O$ in the reaction of 1,2,3,4-tetrahydro-2-phenylisoquinoline with nitromethane revealed that the former was more efficient under the same condition. Moreover, G-RuO_2 NPs catalyst could be easily recycled by filtration. Drawing inspiration from these works, several nanomaterial-based catalytic systems have been developed which showed high catalytic performance in the oxidative aza-Henry (Table 1) and/or oxidative Mannich reactions (Table 2) of tetrahydroisoquinolines. These include: $CuFe_2O_4$ NPs,[13] AuNPore,[14] Fe_3O_4@SiO_2-bipy-[$AuCl_2$][$AuCl_4$],[15] WO_3–W1,[16] sponge AuNPs,[17] MNPs@eosin Y,[18] and Ru@DAFO@ASMNPs.[19] It is worth mentioning that some of these nanocatalyts were also successfully utilized in the cross-dehydrogenative coupling of tertiary amines with various pronucleophiles such as malononitrile, dialkyl malonate, H-phosphonate diesters, trimethylsilyl cyanide, and indole derivatives. However, the scope of tertiary amines are generally limited to the tetrahydroisoquinoline derivatives and therefore expanding the substrate scope of these reactions would be interesting.

The versatile magnetite nanoparticles were also exploited for the cross-dehydrogenative coupling reaction between 4-benzyl-3,4-dihydro-2*H* benzo[*b*][1,4] oxazin-2-one **7** and dimethyl malonate **8**.[20] The reaction was carried out in the presence of a stoichiometric amount of DDQ as oxidant in MeCN at room temperature and provided the coupling product **9** in high yield of 80% (Scheme 4). After completion of the reaction, the catalyst was easily recycled by means of an external magnet and reused seven times with a slight decrease in activity.

Recently, García and Alonso reported an interesting and effective synthetic route to 5,6-dihydroindolo[2,1-*a*]isoquinolines **12** through cross-dehydrogenative coupling of *N*-aryl-1,2,3,4-tetrahydroisoquinolines **10** with nitroalkanes **11** using copper nanoparticles supported on titanium oxide (Cu NPs/TiO_2) as catalyst (Scheme 5).[21] The best conversion efficiency

Table 1 Nanoparticles catalyzed oxidative aza-Henry reactions of tetrahydroisoquinolines with nitroalkanes

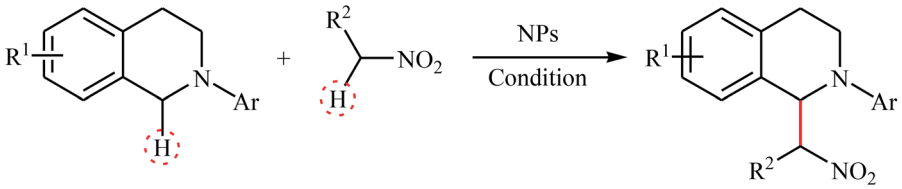

Entry	Catalyst	Conditions	Number of examples	Yield (%)	Ref.
1	$CuFe_2O_4$ NPs	Neat, O_2, 100 °C, 24 h	7	73–92	13
2	AuNPore	Neat, O_2, 80 °C, 24 h	8	70–99	14
3	$[Fe_3O_4@SiO_2$-bipy-$AuCl_2][AuCl_4]$	MeOH, air, 60 °C, 8 h	15	74–91	15
4	WO_3–W1	Neat, O_2, r.t., 24 h	8	70–91	16
5	Sponge AuNPs	H_2O, TBHP, 80 °C, 24 h	10	66–98	17
6	MNPs@eosin Y	DMSO, air, light, 12 h	9	80–92	18
7	Ru@DAFO@ASMNPs	MeOH, air, light, r.t., 12–30 h	6	72–89	19

Table 2 Nanoparticles catalyzed oxidative Mannich reactions of tetrahydroisoquinolines with ketones

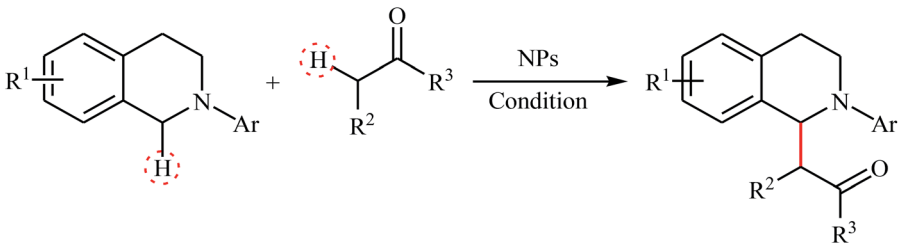

Entry	Catalyst	Conditions	Number of examples	Yield (%)	Ref.
1	$[Fe_3O_4@SiO_2$-bipy-$AuCl_2][AuCl_4]$	AcOH, 4A MS, air, 60 °C, 12 h	12	72–86	15
2	WO_3–W1	MeOH, proline, O_2, light, 24 h	8	70–82	16
3	Ru@DAFO@ASMNPs	MeCN, proline, air, light, 15–24 h	11	69–88	19

was obtained for the reactions containing 1.5 mol% of catalyst at 70 °C under solvent-free conditions. Under optimized conditions, both electron-rich and electron-deficient tetrahydroisoquinoline derivatives were tolerated well and gave the target products in almost fair to excellent yields. However, nitro-substituted tetrahydroisoquinolines were incompatible in this reaction. Of note, the presence of both titanium oxide support and copper nanoparticles were crucial for the success of this transformation. No desired product was found in the absence of any of them. Moreover, the yields in this system were strongly dependent on the temperature, either increase or decrease of the temperature was decreased the reaction efficiency. Mechanistically, a free radical process was likely involved in this reaction (Scheme 6), which could be completely inhibited by

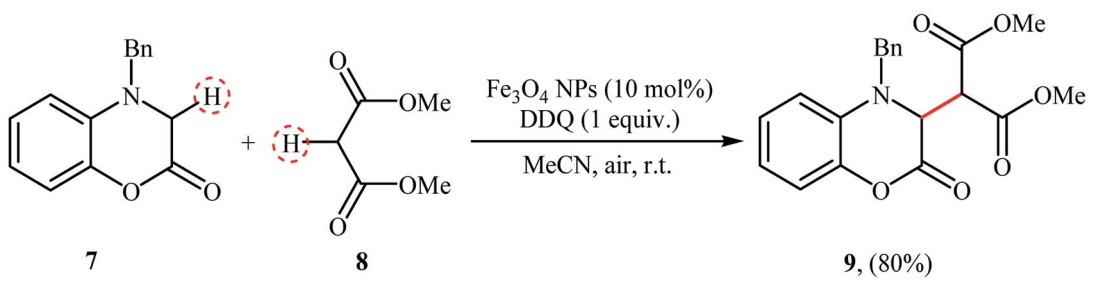

Scheme 4 Fe_3O_4-catalyzed coupling of 3,4-dihydro-1,4-benzoxazin-2-one 7 with malonic ester 8.[20]

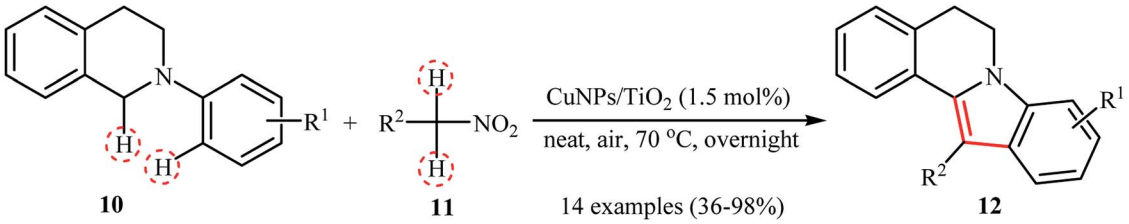

Scheme 5 Synthesis of dihydroindoloisoquinolines **12** through the CuNPs/TiO_2-catalyzed cross-dehydrogenative coupling of tetrahydroisoquinolines **10** and nitroalkanes **11**.[21]

2,2,6,6-tetramethylpiperidine-1-oxyl (TEMPO), a radical scavenger.

3. Constructing $C(sp^3)$–$C(sp^2)$ bonds

The first example of a photocatalytic cross-dehydrogenative coupling reaction employing two different C–H bonds was described in 2013 by Wu *et al.*, who showed that the treatment of *N*-aryl-1,2,3,4-tetrahydroisoquinolines **13** with functionalized indoles **14** in the presence of a combination of eosin Y and graphene-supported RuO_2 nanocomposite (G-RuO_2 NPs) in water under irradiation of visible light (λ > 450 nm) afforded the C3-alkylated indoles **15** with yield ranging from 30% to 98% (Scheme 7).[22] The reaction tolerated a number of important functional groups such as fluoro, chloro, bromo, methoxy, and ester functionalities and promised its potential applications for further manipulation of the final products. However, the reaction failed in the case of a cyano-substituted substrate. Unfortunately, the recyclability/reusability of the catalyst was not explored in this study. To gain insights into the mechanism for this oxidative coupling reaction, kinetic isotope effect experiment was conducted, which revealed that the dissociation of proton from amine was involved in the rate-determining step. In accord to the presumed mechanistic pathway, the reaction starts with the formation of cation radical species **A** *via* a single-electron transfer from tertiary amine **13** to the excited organophotocatalyst [eosin Y]*. Next, this intermediate **A** converts into the iminium ion intermediate **B** through a deprotonation and oxidation sequential process. Subsequently, the nucleophilic addition of indole **14** to this intermediate gives rise to the cross-coupling product **15.** On the other hand, the formed radical anion $[\text{eosin Y}]^{\bullet -}$ is restored to its ground state by G-RuO_2 in water (Scheme 8). Shortly afterwards, Jin and co-workers studied the similar oxidative coupling of tertiary amines with indoles using zero-valent nanoporous gold (AuNPore) as the catalyst and O_2 as an oxidant in refluxing MeOH.[14] Thereby, the corresponding α-indolyl-substituted amines were obtained in moderate to good yields after 24 hours (45–77% for 4 examples). Later, Yan demonstrated that Ru nanoparticles (Ru-NP-1; thickness of 1.4 nm) are also suitable catalysts for the cross-dehydrogenative coupling of *N*-aryl-1,2,3,4-tetrahydroisoquinolines with indoles.[23] Thus, by using 8 mol% of catalyst in binary solvent H_2O/MeOH in a 1 : 1 ratio at room temperature, the desired coupling product were obtained in high yields (up to 98%); however, acidic condition and long reaction

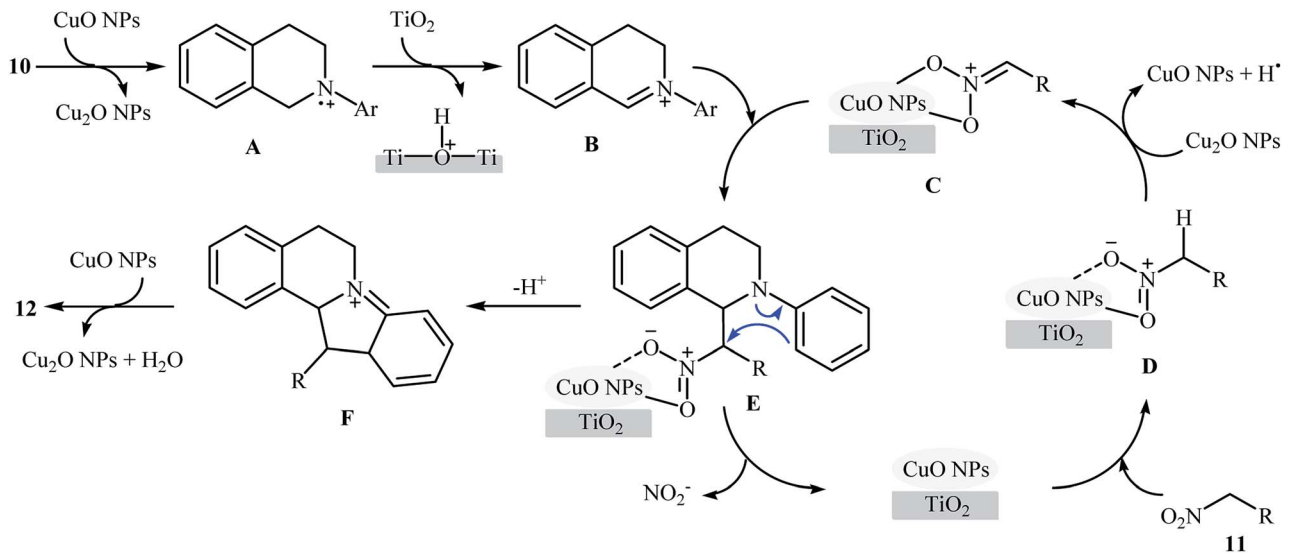

Scheme 6 Proposed mechanism for the formation of dihydroindoloisoquinolines **12**.[21]

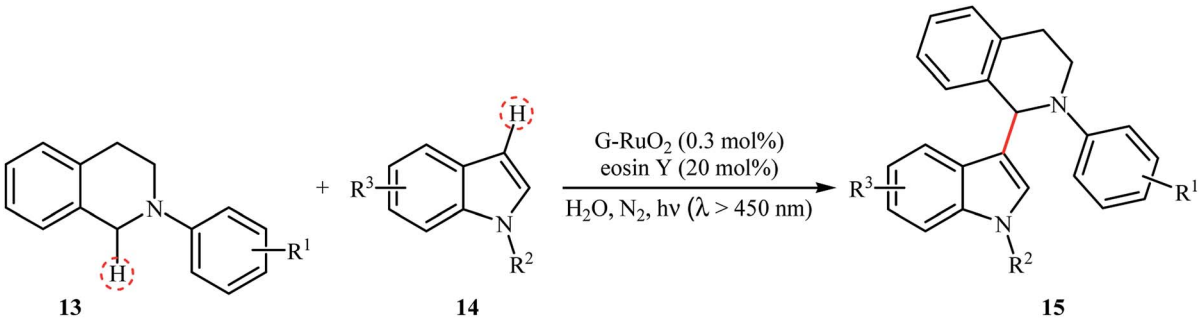

Scheme 7 Wu's synthesis of C3-alkylated indoles **15**.[22]

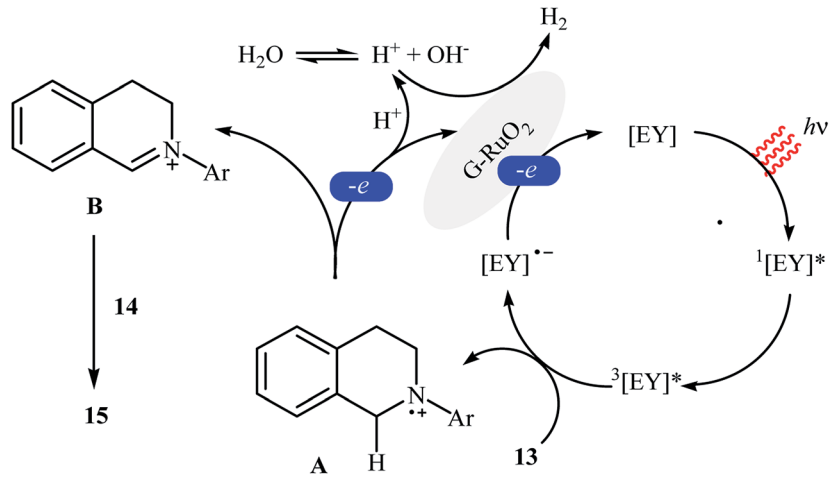

Scheme 8 Suggested mechanism for the reaction in Scheme 7.[22]

time (27–110 h) were necessary. The recyclability of the catalyst was examined, showing a little but noticeable loss in catalytic activity (from 97% in the first run to 77% in the sixth run).

Recently, Yoshida and colleagues disclosed photocatalytic direct cross-dehydrogenative coupling reaction between simple arenes **16** and tetrahydrofuran **17** by using a novel blended catalyst consisting of a TiO_2 photocatalyst and an Al_2O_3-supported PdAu bimetallic catalyst (3–4 nm).[24] The reactions were done under the irradiation of xenon lamp and solvent-free conditions without consuming any oxidizing agent or other additional chemicals; however, only trace amounts of the corresponding α-arylated ethers **18** were obtained (Scheme 9). The conversion and selectivity of the target cross-coupling products heavily depended on the ratio of the two catalytic components, the best results were observed when Pd(2.0)Au(1.0)/Al_2O_3 was used as the catalyst. Noteworthy, compared to the conventional Pd-loaded TiO_2 photocatalyst and the monometallic Pd/Al_2O_3 and Au/Al_2O_3 catalysts, the hybrid catalyst showed superior catalytic activity. In the bimetallic catalyst, electron density being transferred from the Pd atoms to Au atoms and thus the Pd atoms became electron deficient and the Au atoms became electron rich on the support, as indicated by

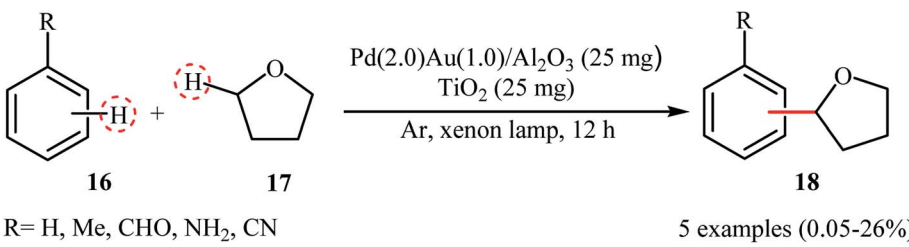

Scheme 9 Dehydrogenative cross-coupling between arenes **16** and tetrahydrofuran **17** reported by Yoshida.[24]

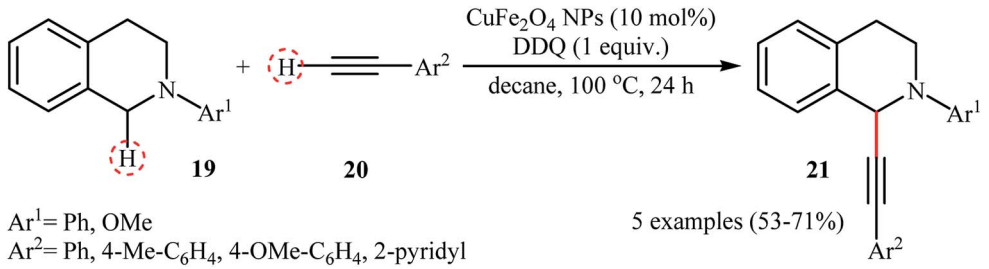

19 **20** **21**

Scheme 10 $CuFe_2O_4$ NPs-catalyzed α-alkynylation of 2-aryl-1,2,3,4-tetrahydroisoquinolines **19** with aromatic alkynes **20** reported by Ramón.[25]

XANES (X-ray absorption near edge structure) analyses of the monometallic and bimetallic samples.

4. Constructing C(sp^3)–C(sp) bonds

Li-Moores and co-workers were among the first to realize cross-dehydrogenative coupling reactions between sp^3-hybridized and sp-hybridized C–H bonds using metal nanoparticles as catalysts.[13] In 2013, they discovered that a magnetic nano-catalyst in combination with an oxidant effects the direct α-alkynylation of 2-aryl-1,2,3,4-tetrahydroisoquinolines **19** with aromatic alkynes **20**, a reaction that has been subject of number of papers in recent years. The best conversion efficiency was obtained for the reactions containing $CuFe_2O_4$ (10 mol%) and DDQ (1 equiv.) in decane at 100 °C. Under optimized conditions, both aromatic and heteroaromatic terminal alkynes were tolerated well and gave the desired coupling products **21** in moderate to good yields (Scheme 10). It is worthwhile to mention that Fe_3O_4 NPs completely failed to promote this transformation. This result clearly showed that the catalytic activity of nano-$CuFe_2O_4$ is due to the presence of copper atoms that able to coordination to the C–C triple bonds and formation of active copper acetylides (Scheme 11). In a similar approach, the Ramón group reported the synthesis of a library of α-alkynylated tetrahydroisoquinoline derivatives utilizing a catalytic amount of iron oxide-supported copper(II) oxide nanoparticles (Fe_3O_4–CuO NPs; 2–4 nm) in a 1 : 2 mixture of choline chloride and ethylene glycol.[25] Of note, other metal oxides impregnated on magnetite such as PdO–Fe_3O_4, Ru_2O_3–Fe_3O_4, NiO–Fe_3O_4, CoO–Fe_3O_4, OsO_2–Fe_3O_4, Ag_2O–Fe_3O_4, Au_2O_3–Fe_3O_4, IrO_2–Fe_3O_4, PtO/PtO_2–Fe_3O_4, WO_3–Fe_3O_4 were also found to promote this reaction, albeit at lower efficiencies. As compared to the heterogeneous Fe_3O_4–CuO catalyst, poorer results were obtained by the CuO and a mixture of CuO and Fe_3O_4. These results indicated that the metal oxide and support in the catalyst play synergistic roles in activating both C(sp^3)–H and C(sp)–H bonds.

In 2015, a related α-alkenylation of tertiary amines with terminal alkynes was reported by Alonso and co-workers.[26] They showed that in the presence of only 1.5 mol% of zeolite Y-supported Cu nanoparticles as the catalyst and *tert*-butyl hydroperoxide (^{t}BuOOH) as an oxidant, reaction of a variety of

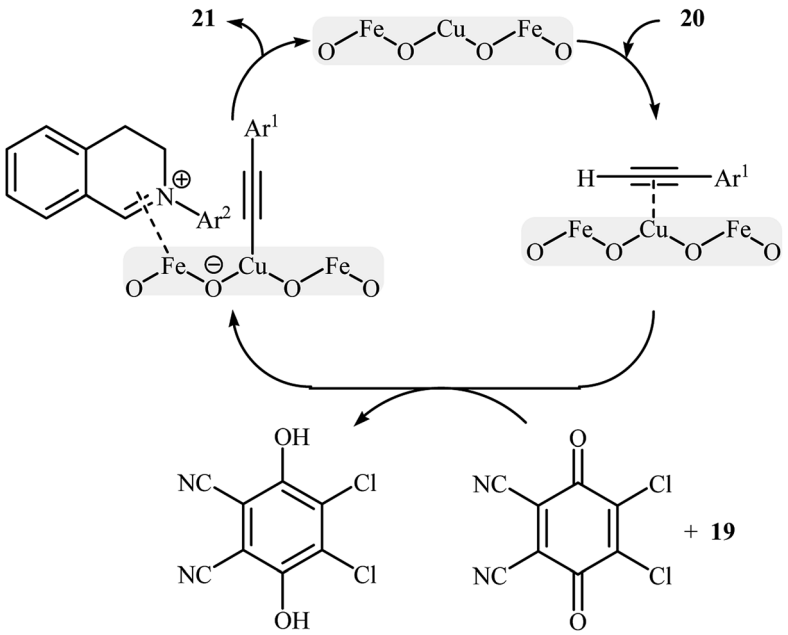

Scheme 11 Proposed mechanism for the reaction in Scheme 10.[25]

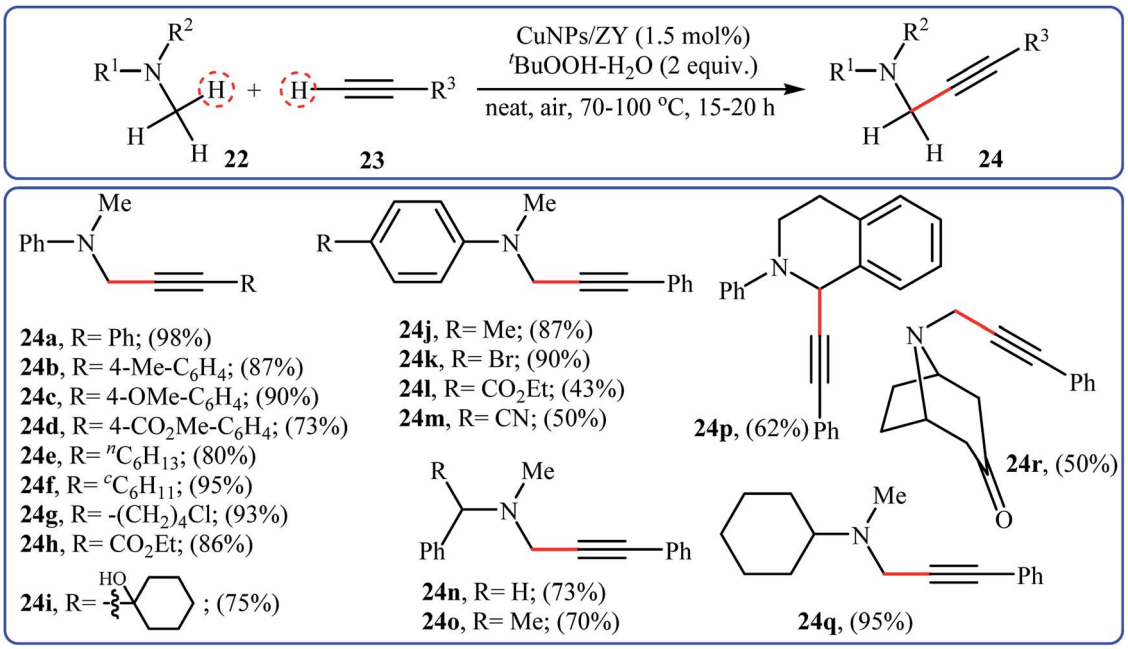

Scheme 12 Cross-dehydrogenative coupling of tertiary amines **22** and terminal alkynes **23** catalyzed by CuNPs/ZY.[26]

tertiary amines **22**, including aromatic, benzylic and aliphatic ones with a wide range of aromatic and aliphatic terminal alkynes **23** under the open air furnished the corresponding α-alkenylated products **24** in moderate to excellent yields (Scheme 12). This synthetic strategy tolerated a number of common functional groups, including chloro, bromo, hydroxy, cyano, ether, ester, and ketone functionalities, and exhibited very high level of regioselectivity. Noteworthy, the reaction can be performed on a gram scale without a significant decrease in yield. Additionally, the catalyst can be reused several times, without loss of reactivity. It should be pointed out that replacing zeolite Y with other supports such as activated carbon, mont K-10, MgO, TiO_2 decreased reaction efficiencies. Later, Jain and Singh along with their co-workers disclosed the alkenylation of benzylic tertiary amines employing $Cu_6Se_{4.5}$ NPs/TBHP combination as a catalytic system under solvent-free condition; however, lower product yields were obtained and higher temperature (100 °C) and an inert atmosphere were required.[27]

Recently, the group of Favier-Gómez's reported the synthesis of ultrafine zero-valent copper nanoparticles (NPs) with mean diameters from about 1.7 to 2.4 nm by decomposition of $[Cu(\kappa^2\text{-}N,N,N',N'\text{-TMEDA})(\mu\text{-OH})]_2Cl_2$ (TMEDA = tetramethylethylenediamine) under hydrogen gas atmosphere (3 atm), in the presence of polyvinylpyrrolidone (PVP) as stabilizer in glycerol (Scheme 13).[28] The catalytic activity was evaluated in the oxidative coupling of tertiary amines **25** with terminal alkynes **26** in the presence of TBHP as an oxidant in glycerol. The obtained results from this study showed that the desired coupling products **27** were formed in moderate to excellent isolated yields (Scheme 14). The best results were obtained for aromatic tertiary amines. The prepared Cu NPs was also successfully applied as a catalyst for one-pot construction of synthetically important propargylic amines,[29] through the A^3 coupling reaction of amines, aldehydes, and terminal alkynes.

5. Constructing C(sp^2)–C(sp^2) bonds

5.1. C(aryl)–C(aryl) bonds

Biaryls are the core structure of many natural products and commercialized drugs such as imatinib, losartan, felbinac, febuxostat, and telmisartan.[30] Additionally, they are widely found in agrochemicals, liquid crystals, and ligands.[30,31] In light of the widespread biological activities of functionalized biaryls, numerous synthetic methods have been developed for their preparation which the majority of them relying on the known C–C cross-coupling reactions, including Ullmann, Suzuki, Hiyama, Negishi, stille, and Kumada–Corriu reactions.[5b,c,30–34]

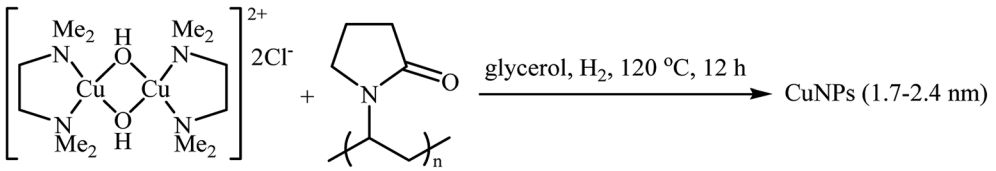

Scheme 13 Preparation of CuNPs reported by Favier and Gómez.[28]

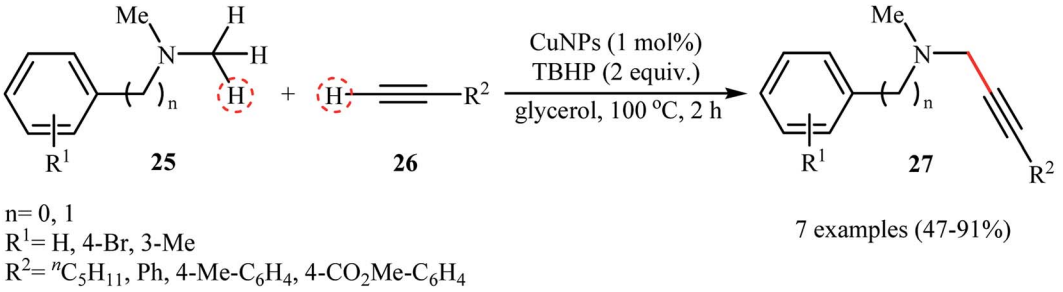

Scheme 14 Copper(0) nanoparticles catalyzed coupling of C(sp^3)–H bonds with C(sp)–H bonds.[28]

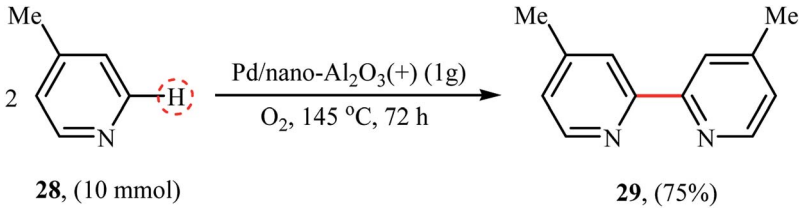

Scheme 15 Pd/nano-Al_2O_3(+)-catalyzed homo-coupling of 4-methyl pyridine **28**.[36]

Unfortunately, all of these methods relied on the use of pre-functionalized coupling partners, which limit their range of applications. An alternative protocol for the construction of the titled scaffolds involves the oxidative coupling between two C(sp^2)–H bonds.[35] Although several efficient catalytic systems have been developed, the application of nanoparticles as catalysts for this reaction is a new research area and thus scarcely studied.

In 2008, the first biaryl synthesis by double C–H bond coupling over heterogeneous metal nanoparticles was reported by Neal and Weaver.[36] Several nano alumina-supported palladium catalysts were tested for the synthesis of 4,4′-dimethyl-2,2′-bipyridine **29** from 4-methyl pyridine **28** and Pd/nano-Al_2O_3(+) catalysts prepared *via* the precipitation method afforded the highest yield (Scheme 15). Interestingly, the catalytic activity was very dependent on the catalyst preparation methods, the catalyst prepared *via* the wet impregnation method exhibited poor activities in this reaction compared to the one prepared *via* the precipitation method. Additionally, the catalysts prepared using another alumina nanoparticles (*e.g.*, nano-Al_2O_3(−) and γ-Al_2O_3) did not exhibit significant activities in the reaction and the commercial Pd/Al_2O_3 was found to be almost inactive catalyst.

Six years later, Ishida and Tokunaga along with their co-workers describe that ZrO_2-supported $Pd(OH)_2$ nanoparticles (1.8 ± 0.9 nm) can be used as effective heterogeneous catalysts for the C(aryl)–C(ary) bonds formation *via* double C(aryl)–H bond functionalization.[37] 10 wt% of catalyst has been utilized in the oxidative intramolecular coupling of diarylamines **30** in a 1 : 1 mixture of AcOH/1,4-dioxane under oxygen atmosphere to give the corresponding carbazoles **31** in poor to high yields, ranging from 8% to 85% (Scheme 16). The results demonstrated that the electronic character of the substituents on the aryl rings had a high impact on the facility of the reaction. Generally, the electron-rich diarylamines afforded better yields compared to the electron-deficient ones. Moreover, the outcome of the reaction was strongly dependent on the substitution pattern of the starting material. For example, 3-methoxydiphenylamine was more reactive than 4-methoxydiphenylamine. The authors described this fact by high electron density of *m*-methoxydiphenylamine at the *o*,*p*-positions which accelerate the attack by electron-deficient Pd(II) species. It should be mentioned that the catalyst were also

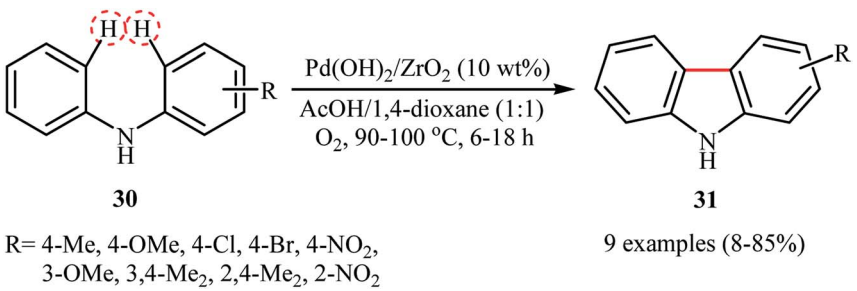

Scheme 16 Synthesis of carbazoles **31** from the corresponding diarylamines **30** through the double C(aryl)–H bond functionalization.[37]

Table 3 AuNPs/TiO_2-catalyzed oxidative C–H/C–H homocoupling of aromatic compounds **32**

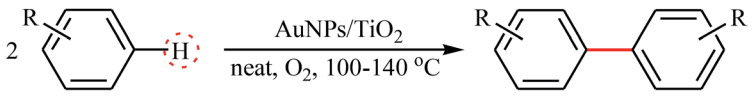

32 **33**

Entry	R	Au/arene (mol ratio × 100)	TOF[a]	TON[b]	Selectivity (%)
1	H	0.022	382	230	99
2	Me	0.026	176	206	98
3	1,5-Me_2	0.030	18	71	98
4	1,2,6-Me_3	0.034	6	8	98
5	Cl	0.032	368	88	99
6	NO_2	0.035	176	175	99
7	OH	0.027	85	336	80

[a] Turnover frequency (TOF). [b] Turnover number (TON).

found to be highly efficient for the synthesis of dibenzofurans from the corresponding diarylethers.

Similar to PdNPs-catalyzed double C(aryl)–H bond coupling reactions, a few AuNPs-catalyzed reactions were also reported in literature. In 2014, Serna and Corma reported the successful use of AuNPs/TiO_2 in the waste-free preparation of biaryls **33** from the corresponding aryl molecules **32** using molecular oxygen as the sole oxidant under solvent-free conditions (Table 3).[38,39] Noteworthy, the particle size of supported gold strongly influences the activity of catalyst. The highest catalytic activity was observed for gold crystallites of ~3 nm diameter.

Another (Au NP)-based catalyst, *i.e.*, Au/Co_3O_4, was also found to be active towards the oxidative coupling of simple arenes.[40] The reactions were occurred in AcOH under 1.5 MPa pressure of O_2 at 100–150 °C. Although a series of functionalized biaryls were obtained in good yields, the procedure was not general and several substrates (*e.g.*, 1,4-di-*tert*-butylbenzene, methyl benzoate, dimethyl terephthalate, 1-(trifluoromethyl) benzene) failed to participate in this reaction or afforded only a trace amount of the target products. Based on a series of control experiments, the authors suggested that the reaction proceeds by an electrophilic aromatic substitution pathway as depicted in Scheme 17.

Very recently, Cravotto and co-workers prepared Pd cross-linked β-cyclodextrin (Pd/CβCAT) as a green heterogeneous catalyst for the MW-assisted cross-dehydrogenative coupling of arenes.[41] In the presence of 10 mol% of catalyst, 30 mol% of pivalic acid (PivOH), and 2 equiv. of $AgNO_3$, benzo[*d*]thiazole **34** react with 2-methylthiophene **35** in γ-valerolactone (GVL) at 140 °C to provide the C-2 heteroarylated product **36** in 95% yield (Scheme 18). DMA was also found to be useful solvent for this transformation. However, other solvents like ethyl lactate, ethyl levulinate were not so effective like GVL or DMA. Unfortunately, recycling test of the catalyst indicated a strong decrease in activity after each reaction cycle, as the conversion drops dramatically from 95% to 15% in the sixth cycle.

5.2. C(aryl)–C(alkenyl) bonds

The transition-metal-catalyzed dehydrogenative Heck reaction (Fujiwara–Moritani reaction) is one of the most straightforward and economical protocols for the construction of olefination products.[42] Over the years, numerous excellent catalytic system have been developed for this elegant C–C bond forming reaction.[43] Despite their benefits, usually they require the addition of co-catalysts, ligands, and/or additives, which may limit the application of this interesting page of C–C bond formation more or less. In 2011, Ying and colleagues developed a highly active and reusable palladium-polyoxometalate nanocatalyst with the formula Pd–$H_6PV_3Mo_9O_{40}$/C for the efficient oxidative olefination of anilides **37** with acrylates **38**, using O_2 as the terminal oxidant to produce substituted anilides **39** under relatively mild conditions (Scheme 19).[44] The results revealed that the process strongly depended on the electronic nature of the anilides, with the best yields were obtained with unsubstituted or with monomethylated substrates. The same catalytic system was also applied to the oxidative C–H/N–H cross-coupling of various acrylates with secondary amines, and the corresponding products were obtained in high yields (up to 90%). The presence of polyoxometalate was crucial for the oxidative C–C and C–N coupling reactions since it served as a reoxidation catalyst under O_2. The catalyst could be recycled several times with only a minor loss in its activity and without any change in the size of the Pd NPs as confirmed by their TEM images (Fig. 2).

Recently, silver–palladium alloy nanoparticles anchored on reduced graphene oxide (Ag_1Pd_1-rGO) was used as efficient and recyclable catalyst for the chelation-assisted *ortho* C–H bond olefination of aromatic amides **40** with acrylates **41** by Hu *et al.*[45] The reactions take place in the presence of benzoquinone (BQ) as an oxidant in DCE at 100 °C under an air atmosphere and afforded the target coupling products **42** in moderate to high yields within 12 h (Scheme 20). It is worth mentioning that the use of two-fold of acrylate for an extended time (24 h) led to di-

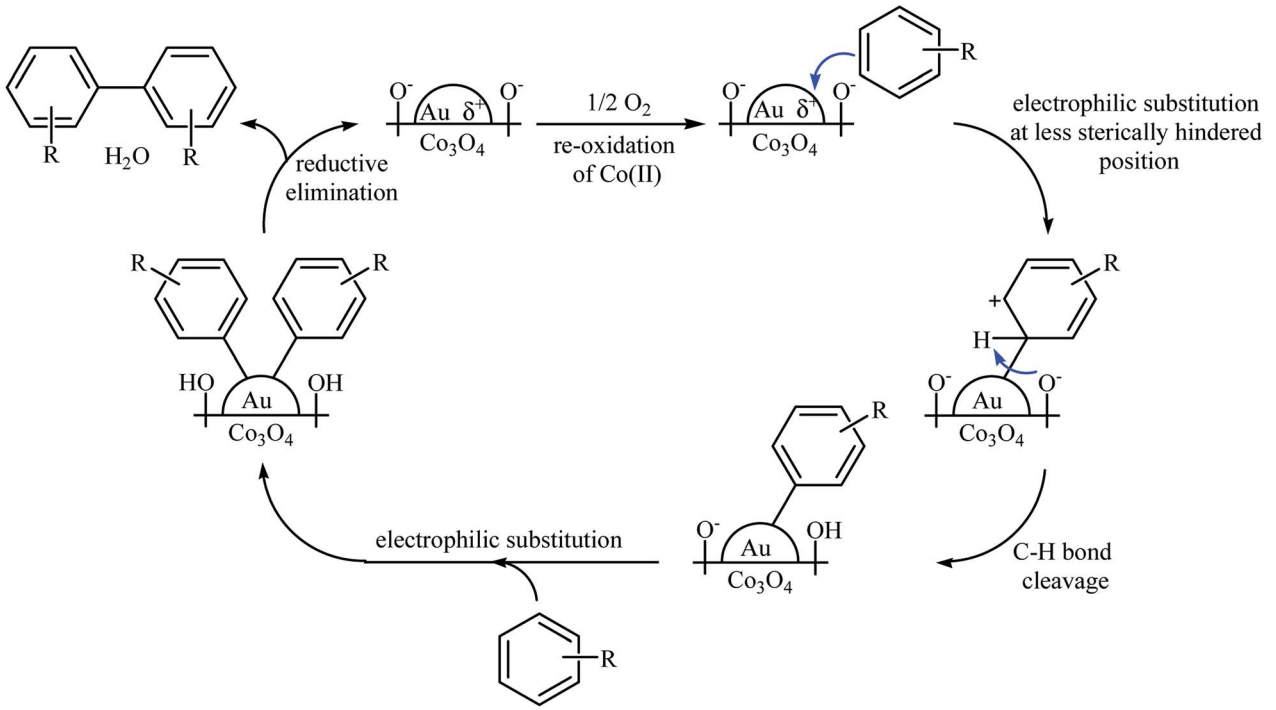

Scheme 17 Plausible reaction mechanism for the oxidative coupling of aromatic compounds over Au/Co_3O_4.[40]

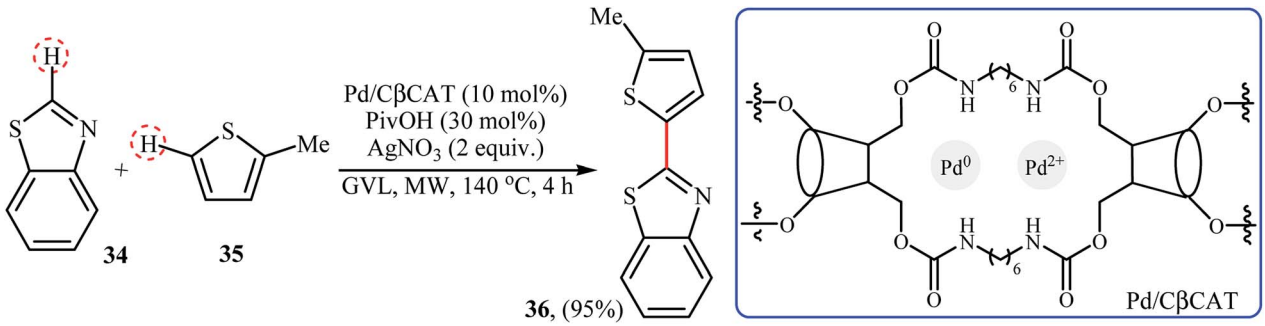

Scheme 18 Coupling of benzo[*d*]thiazole **34** with 2-methylthiophene **35** reported by Cravotto.[41]

olefinated products in good to excellent yields. Noteworthy, the catalyst could be reused for five consecutive runs, with only negligible loss of activity. The authors found that Ag and Pd atoms in the alloy nanoparticles play synergistic roles in the catalytic activity. Investigation revealed that Pd-rGO had very low catalytic activity than Ag_1Pd_1-rGO and Ag-rGO was catalytically inert for this C–C coupling reaction. Mechanistic investigations revealed that the transformation possibly proceeds

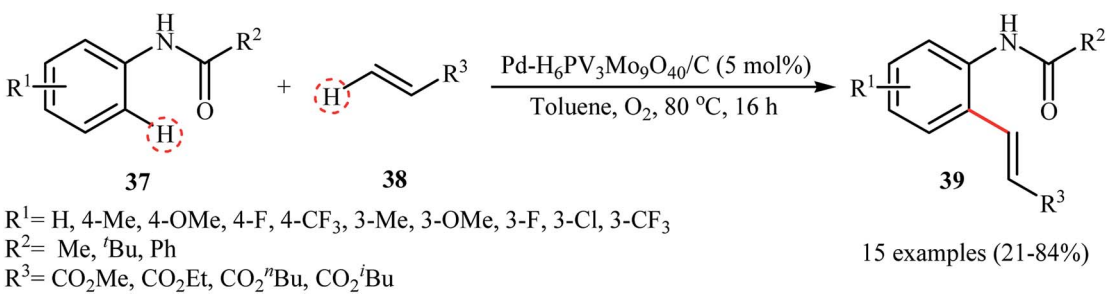

Scheme 19 PdNPs-catalyzed dehydrogenative Heck reaction.[44]

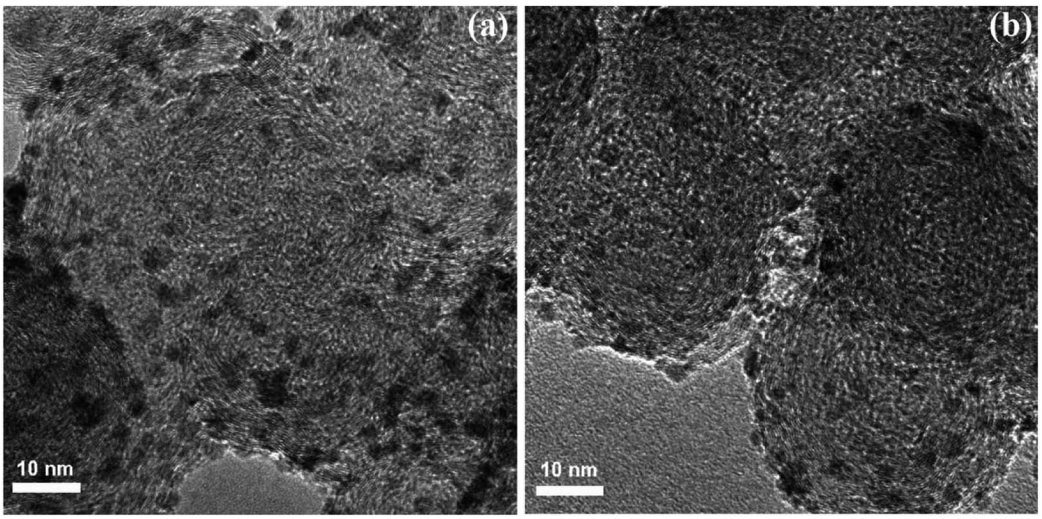

Fig. 2 TEM images of Pd-PV_3Mo_9/C (a) before and (b) after the first recycle of the C–C coupling reaction.[44]

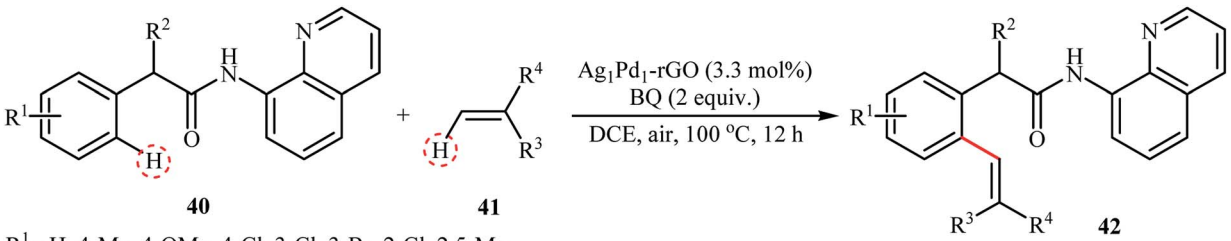

R^1= H, 4-Me, 4-OMe, 4-Cl, 3-Cl, 3-Br, 2-Cl, 2,5-Me_2
R^2= H, Me, Et
R^3= H, Me
R^4= CO_2Me, CO_2Et, $CO_2{}^nBu$, $CO_2{}^iBu$, $CO_2{}^nBu$, SO_2Ph, $CONMe_2$

Scheme 20 Direct C–H bond olefination of amides **40** with acrylates **41** catalyzed by Ag_1Pd_1-rGO.[45]

though the following key steps (Scheme 21): (i) coordination of the Pd atoms of the catalyst to the two nitrogen atoms of the amide **40** to produce intermediate **A;** (ii) oxidation of **A** by BQ and air to afford intermediate **B;** (iii) coordination of the *in situ*-formed Pd(II) species with the intramolecular aminoquinoline along with the loss of the hydroquinone to form cyclopalladated intermediate **C;** (iv) coordination of intermediate **C** to the olefin **41** to give intermediate **D;** (v) insertion of the C=C bond into the C–Pd bond to yield intermediate **E;** and (vi) β-hydride elimination of the alkylpalladium intermediate **E** to form the expected products **42.**

5.3. C(aryl)–C(aldehyde) bonds

The wide importance of diaryl ketones as intermediates in the synthesis of valuable industrial products such as pharmaceuticals, agrochemicals, fragrances, flavors, and dyes,[46] stimulates researchers for develop more efficient and simple methods for their preparation. Among numerous known methodologies for diaryl ketone synthesis, the most green and straightforward procedure is cross-dehydrogenative-coupling reactions between arenes and arenecarbaldehydes.[47] In 2013, Ramani and co-workers reported for the first time the usefulness of metal nanoparticles as catalysts for the oxidative cross-coupling of simple arenes with aromatic dehydes.[48] They used the Fe_3O_4 magnetic nanoparticles (10–30 nm) to promote the *ortho*-benzoylation of phenols **43** with aromatic aldehydes **44** utilizing K_2CO_3 as an inexpensive base and air as the terminal oxidant (Scheme 22). The reaction proved to be efficient on a variety of electron-rich and electron-poor aldehydes, affording exclusively the *ortho*-benzoylated products **45.** However, the reaction did not work with electron-poor phenols. Interestingly, when 2-substituted (NO_2, Cl, Br) arenecarbaldehydes were treated with phenols under the standard condition, biologically important xanthones were obtained in good yields (55–72% for 6 examples) in one step *via* a double C–H bond coupling. Shortly afterwards, Gerbino's research team improved the efficiency of this reaction by performing the process in the presence of a low loading (0.9 mol%) of CuNPs supported on silica coated maghemite (CuNPs/MagSilica) as a magnetically retrievable catalyst.[49]

Recently, Liu and Zhang used their Ag_1Pd_1 nanoparticle-reduced graphene oxide nanocomposite as a catalyst for the acylation of 2-arylpyridines **46** with aldehydes **47.**[50] The reaction was conducted using *tert*-butyl hydroperoxide (TBHP) as an

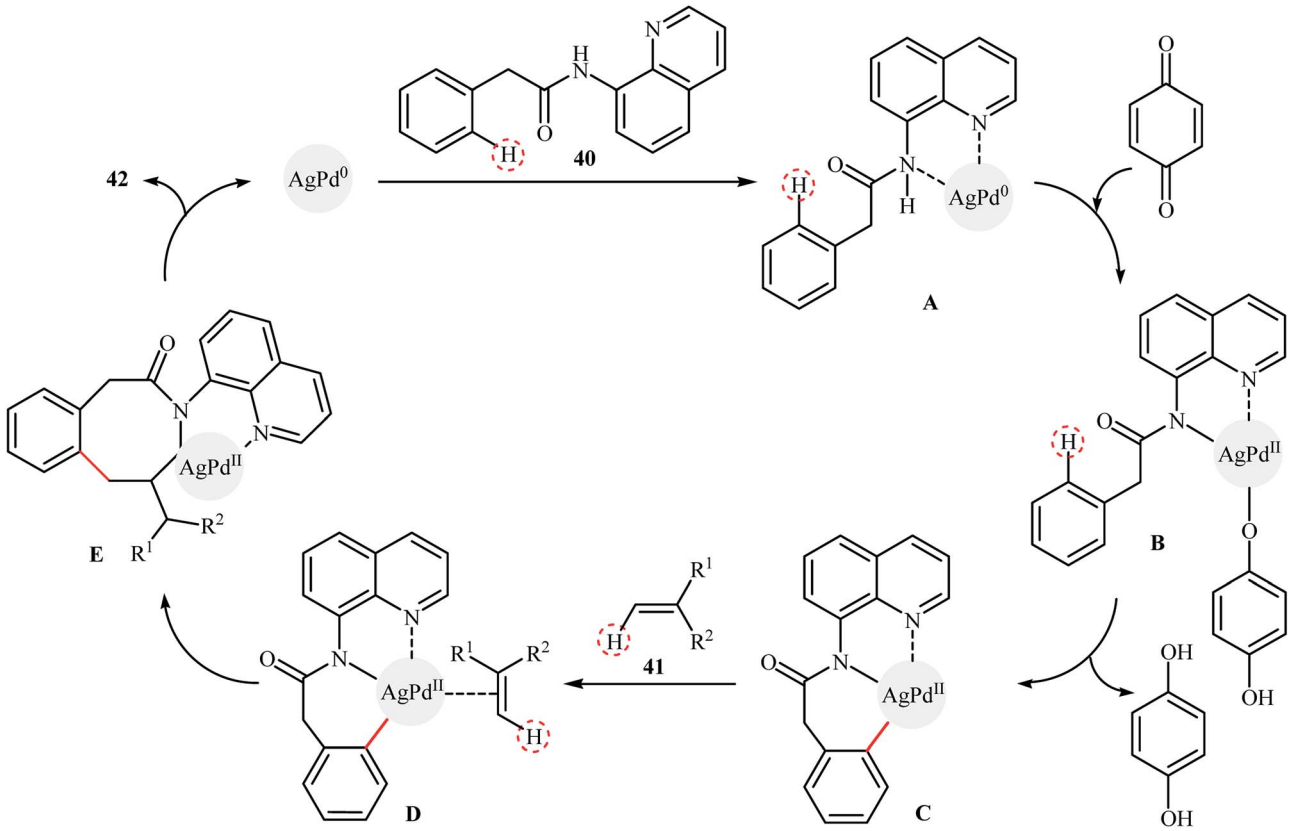

Scheme 21 The possible mechanism of Ag_1Pd_1-rGO-catalyzed olefination of aromatic amides **40**.[45]

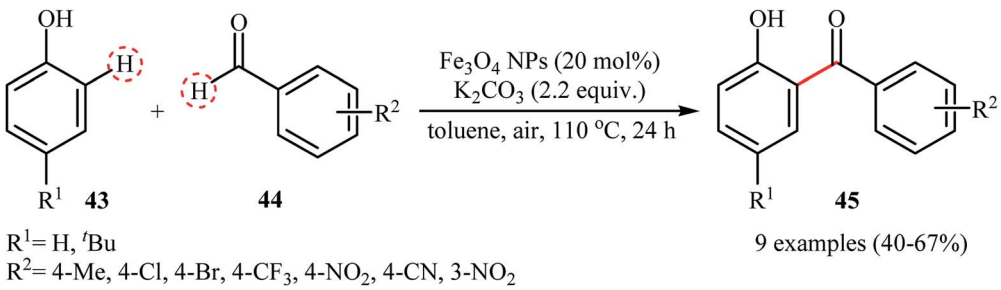

Scheme 22 Synthesis of *ortho*-hydroxybenzophenones **45** catalyzed by Fe_3O_4 NPs.[48]

oxidant under an air atmosphere and afforded the diaryl ketones products **48** in good to high yields (Scheme 23). Applying this method, aliphatic aldehydes could also be arylated in moderate yields. Of note, the catalyst could be reused at least for five times with only 9% decline in the activity. The authors proposed mechanism for this transformation is analogous to the one depicted for cross-dehydrogenative Heck reaction in Scheme 21.

6. Constructing C(sp^2)–C(sp) bonds

In 2016, Kaur, Kumar and Bhalla reported about the use of CuNPs (8–20 nm) in combination with supramolecular aggregate of triazole *N*-oxide appended perylene bisimide (PBI) derivative **49** (**49**: CuNPs) as a highly active photocatalytic system for *ortho*-selective mono-alkynylation of oxazoline substituted benzamide derivative **50** with terminal alkynes **51** under irradiation of visible light. The results demonstrated that the desired internal alkynes **52** were slowly formed in moderate to good yields at room temperature under an atmosphere of air (Scheme 24). Various aliphatic, aromatic and heteroaromatic terminal alkynes were utilized to establish the general applicability of this synthetic process. It should be mentioned that the recycling test showed a small loss of catalytic activity from 72% in the 1st run to 56% in the 4th run. To the best of our knowledge, this is only reported example on the utilization of nanocatalysts in direct C(sp^2)–C(sp) bonds forming reactions.

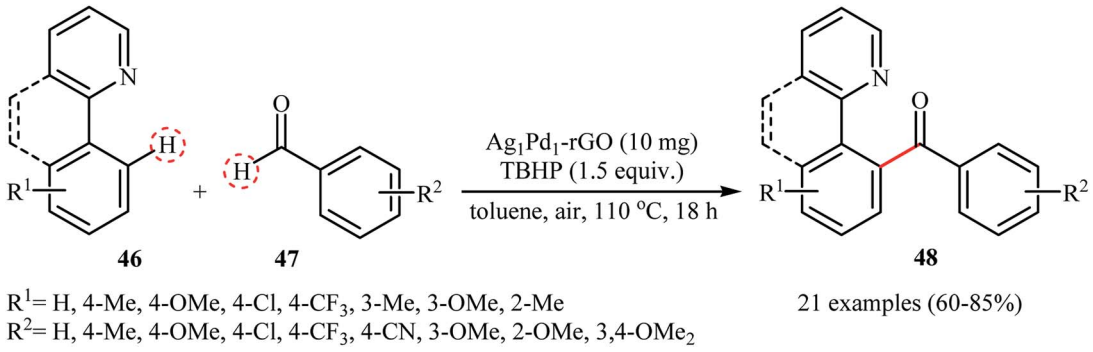

Scheme 23 Ag_1Pd_1-rGO-catalyzed cross-dehydrogenative coupling of 2-arylpyridines **46** with aromatic aldehydes **47**.[50]

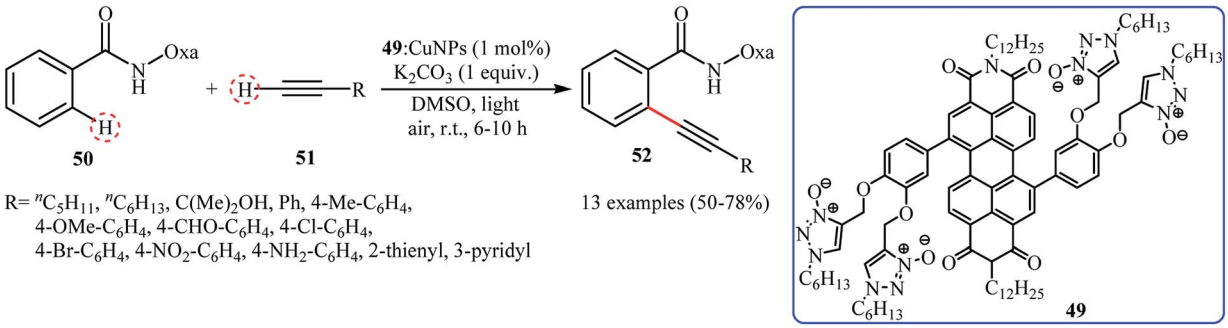

Scheme 24 *Ortho*-selective alkynylation of oxazoline substituted benzamide **50** with terminal alkynes **51** catalyzed by **49**: CuNPs.[51]

7. Constructing C(sp)–C(sp) bonds

1,3-Diynes are not only omnipresent in bioactive nature products,[52] but also paramount important building blocks in organic synthesis.[53] Without slight doubt, the most straightforward approach to the synthesis of symmetrical 1,3-diynes is the oxidative homo-coupling of two terminal alkynes, which known as the Glaser coupling.[54] Although numerous efficient metal nanocatalysts have been reported for this interesting and useful reaction (Table 4),[55–70] the nanometal-catalyzed hetero-coupling reactions between two different alkynes were less developed. Noteworthy, due to the competitive reaction pathways between homo-coupling and hetero-coupling reactions, synthesis of unsymmetrical 1,3-diynes is more difficult compared to the symmetrical ones.[71]

One of the earliest reports on the utilization of nanostructured catalysts in cross-dehydrogenative coupling reactions between two different terminal alkynes was published by Corma and colleagues in 2016,[72] who showed that the treatment of terminal alkyne molecules **53** with **54** in the presence of a catalytic amount of TiO_2-supported CuO_x NPs (~2 nm) under an oxygen atmosphere, resulted in the formation of the corresponding unsymmetrical 1,3-diynes **55** in good to excellent yields, ranging from 61% to 92% (Scheme 25). Interestingly, both aliphatic and aromatic terminal alkynes were compatible with this challenging reaction. Concurrently, Tang and Liu along with their co-workers reported an example of unsymmetrical 1,3-diyne synthesis *via* the reaction of phenylacetylene with 4-methoxyphenylacetylene using 10 mol% of Cu_2O NPs as catalyst in a binary solvent H_2O/TBAB (tetrabutylammonium bromide) in a 1 : 4 ratio.[56] However, the target diyne was isolated in only 30% yield along with a mixture of both possible homo-coupling products.

In the same year, the group of Rossi-Suib prepared thermally stable mesoporous copper oxide supported manganese oxide nanoparticles with Mn/Cu molar ratio 10/1 through the reaction of $Cu(NO_3)_2 \cdot 3H_2O$ with $Mn(NO_3)_2 \cdot 4H_2O$ in the presence of P123 ($PEO_{20}PPO_{70}PEO_{20}$) as a pluoronic surfactant in acidic ^{n}BuOH.[58] The prepared material (*meso* Cu/MnO_x) exhibits a large surface area of over 270 $m^2\ g^{-1}$ and uniform mesoporous size (3.0–3.4 nm) distribution. The authors demonstrated that their heterogeneous catalyst can effectively promote the oxidative coupling reactions of two different terminal alkynes **56** and **57** to furnish the corresponding 1,3-diyne products **58** in moderate yields (Scheme 26). Noteworthy, the catalyst can be readily separated by simple filtration and reused over 8 reaction cycles without a significant decrease in activity. Moreover, no change in the PXRD (powder X-ray diffraction) pattern after the 8th cycle was observed, which confirms that the catalyst can retain the crystal structure even after multiple reuse cycles.

Following these reports, sub-nanometer ($d = 0.8 \pm 0.2$ nm) gold particles supported on 3-aminopropyl-functionalized silicate SBA-15 (Au/SBA-15-amine) was successfully used as recyclable catalyst for high yielding synthesis of unsymmetrical 1,3-diynes **61** from the reaction of 4-methoxyphenylacetylene **59** with aromatic terminal alkynes **60** at room temperature.[73] Better

Table 4 Glaser homocoupling reactions catalyzed by nanosized metals[a]

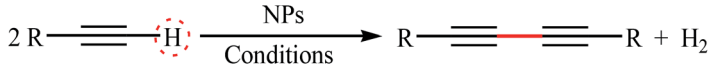

Entry	Catalyst	Conditions	Number of examples	Yield (%)	Ref.
1	CuNPs	THF, 66 °C, 8–24 h	11	65–90	55
2	Cu_2O NPa	TBAB/H_2O, 60 °C, 14–24 h	12	33–93	56
3	CuNPs/TiO_2	THF, 65 °C, 2–24 h	16	60–96	57
4	CuNPs/MnO_x	Toluene, 105 °C, 1–12 h	13	82–98	58
5	Resin-CuNPs	DMSO, 50 °C, 8 h	7	90–95	59
6	CuNPs-HAp	MeCN, reflux, 72 h	8	21–99	60
7	Cu/Cu_2ONPs@GO	EtOH, 80 °C, 8 h	12	53–99	61
8	SBA-15@DABCO-Pd	MeCN, CuI, r.t., 5–24 h	9	62–94	62
9	PdNPs@$Al(OH)_3$	DMSO, NaOAc, Ag_2SO_4, 90 °C, 8–48 h	11	50–99	63
10	AuNPs@C	1,3-DCB, 170 °C, 18 h	10	60–90	64
11	Ni-MINT	Me_2O/H_2O, DABCO, 140–170 °C, 15–45 min	6	51–90	65
12	AgNPs@g-C_3N_4	EtOH/H_2O, MW, 80 °C, 18–20 min	9	94–98	66
13	CuNPs/MagSilica	THF, 66 °C, 2–24 h	7	58–95	67
14	CuO–Fe_3O_4	Neat, ^{t}BuOK, 60 °C, 2–7 h	14	20–99	68
15	Fe_3O_4@SiO_2@APTMS@$Cu(en)_2$	DMF, Na_2CO_3, 80 °C, 15–60 min	4	86–100	69
16	Pd_2Au/mpg-C_3N_4	DMF, 100 °C, 12–16 h	7	71–99	70

[a] Number of examples.

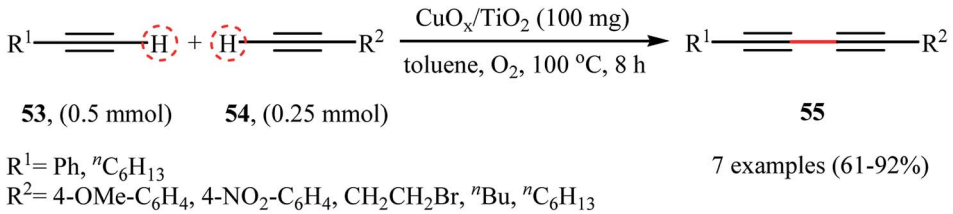

Scheme 25 CuO_x/TiO_2-catalyzed hetero-coupling of **53** with **54**.[72]

results were observed when commercially available λ^3-iodane $PhI(OAc)_2$ was used as the oxidant and 1,10-phenanthroline as additive (Scheme 27a). Under the optimized reaction conditions and by using a catalyst loading of 5 mol%, a library of symmetrical 1,3-diynes were also obtained in excellent yields (up to 98%) from the corresponding terminal alkynes. Magnetically separable nano-$CuFe_2O_4$ (with an average particle size of 30–35 nm) was also found to be active catalyst towards the oxidative cross-coupling of aromatic alkynes **62** with terminal alkynes **63** at room temperature.[74] The reaction was performed under open air using pyrrolidine as a base, tolerated a number of important functional groups (*e.g.*, F, Cl, Br, OMe, CO_2Me, and OH), and provided the expected 1,3-diynes **64** in moderate yields (Scheme 27). Interestingly, the catalyst can be easily separated from the reaction mixture by using an external magnetic field, and its efficiency remains unchanged even after recycling over five runs.

Very recently, Vinod and Vaidhyanathan's research team prepared a novel phenol-pyridyl covalent organic framework (IISERP-COF9) supported Cu/Cu_2O nanoparticles (Cu@IISERP-COF9) through the condensation of 4,4′,4″-(pyridine-2,4,6-triyl) trianiline with 2-hydroxybenzene-1,3,5-tricarbaldehyde in the

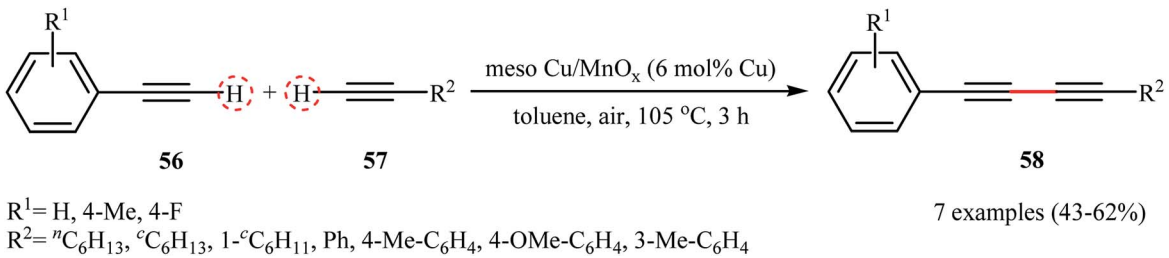

Scheme 26 Cross-dehydrogenative coupling of terminal alkynes **56** with **57** catalyzed by *meso* Cu/MnO_x.[58]

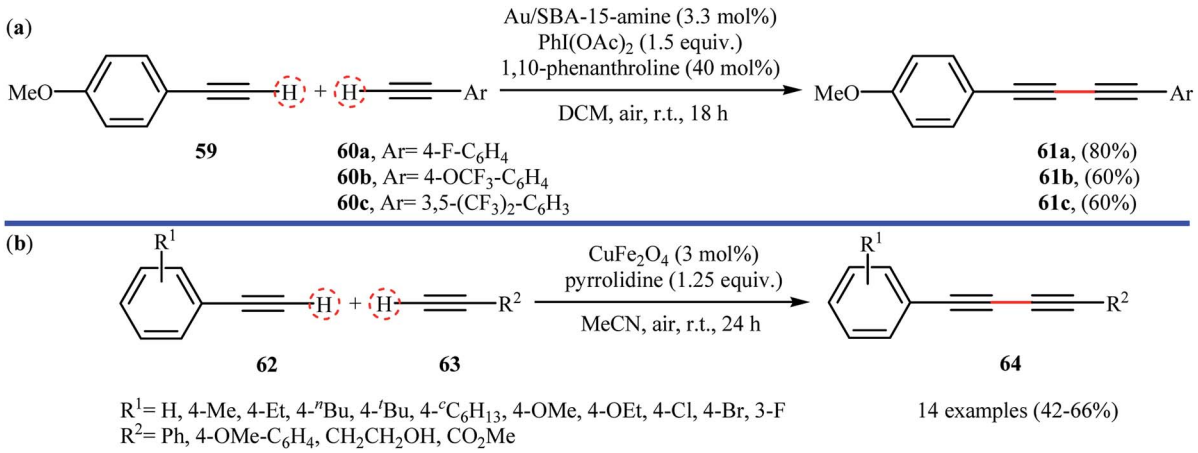

Scheme 27 (a) Oxidative cross-coupling of 4-methoxyphenylacetylene **59** with aromatic terminal alkynes **60** catalyzed by Au/SBA-15-amine;[73] (b) $CuFe_2O_4$-catalyzed cross-dehydrogenative coupling of **62** with **63**.[74]

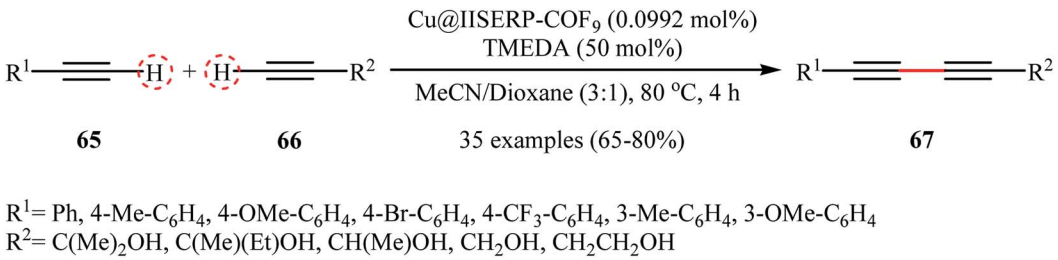

Scheme 28 Vinod–Vaidhyanathan's synthesis of unsymmetrical 1,3-diynes **67**.[75]

binary solvent DCB-BuOH at 120 °C, followed by stirring of the resulting COF with $CuCl_2$ in the presence of ascorbic acid in THF at 80 °C.[75] The catalytic activity of the synthesized composite has been evaluated in the cross-dehydrogenative coupling of a range of aromatic terminal alkynes **65** with aliphatic alkynes **66** in the presence of tetramethylethylenediamine (TMEDA) as a base in a 3 : 1 mixture of $CHCl_3$/dioxane. Good to high yields of the target unsymmetrical 1,3-diynes **67** were obtained within 4 h at 80 °C (Scheme 28). Recycling tests indicate that the catalyst can be reused in five consecutive trials with only a slight decrease in activity. A possible mechanism for the formation of 1,3-diynes **67** was given by this report (Scheme 29), which involves the initial formation of the Cu(II) species **A** through the oxidative addition of the carbon–halogen bond of $CHCl_3$ to the Cu center of the catalyst, followed by its ligand exchange with the alkynes **65** and **66** to form a copper diacetylide complex **B**, which after oxidation in the

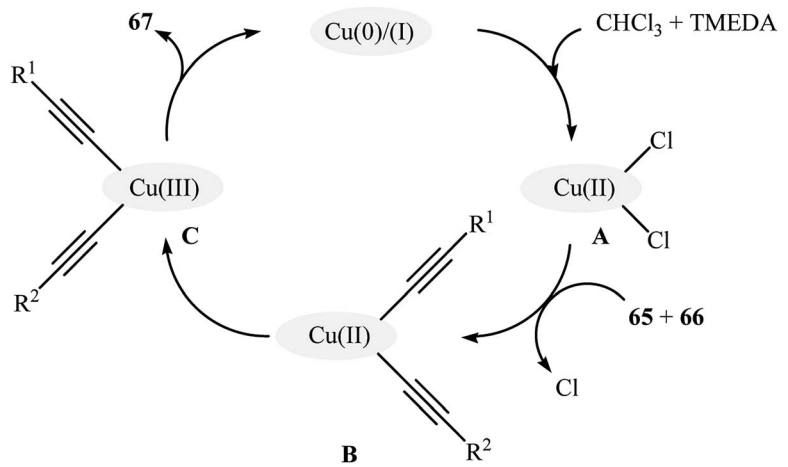

Scheme 29 Plausible mechanism for the hetero-coupling of aromatic terminal alkynes **65** with aliphatic terminal alkynes **66**.[75]

presence of air converts to the Cu(III) complex **C**. Finally, the reductive elimination of this intermediate **C** affords the observed 1,3-diynes **67** and regenerates the catalyst.

8. Conclusion

Over the past few years, the construction of C–C bonds through the direct oxidative coupling of two different C–H bonds between two reactants have attracted considerable attention as cleaner and more sustainable synthetic alternative to traditional coupling procedures which rely on the use of pre-functionalized starting materials. However, the control of regioselectivity in these reactions is a great challenge because C–H bonds are ubiquitous in organic molecules. There are two major strategies for control of selectivity: (i) directing group-based and (ii) catalyst-based controls. However, the requirement of installing and then removing the directing groups limited the application of the former strategy. As illustrated, the use of nanostructured catalysts allow the highly selective cross-dehydrogenative coupling between two C–H bonds, with the benefits of high product yield and ease of catalyst separation, recovery, and recycling. Interestingly, all the six kinds of C–C bonds [*i.e.*, $C(sp^3)$–$C(sp^3)$, $C(sp^3)$–$C(sp^2)$, $C(sp^3)$–C(sp), $C(sp^2)$–$C(sp^2)$, $C(sp^2)$–C(sp), C(sp)–C(sp)] were successfully fabricated by nanoparticles catalyzed oxidative coupling of the corresponding C–H bonds. Noteworthy, some of the reactions covered in this review could be easily scaled up to provide multi-gram quantities of the desired coupling products. This results clearly show the potential application of nanocatalyzed cross-dehydrogenative coupling reactions in industry. Despite the remarkable accomplishments during the past few years in this interesting research arena, many challenges still remain to be overcome: (i) most of the covered reactions in this review have been performed at high temperatures. Thus, there is a further need for investigation and discovery of novel catalytic systems, which can allow these reactions under milder conditions; (ii) the substrate scope in some reactions such as $C(sp^3)$–H/$C(sp^3)$–H couplings are narrow and therefore, of course, expanding of the substrate scope of these reactions are necessary; and (iii) the application of tri-metallic and multi-metallic nanoparticles in these reactions should be investigated.

Conflicts of interest

There are no conflicts to declare.

Acknowledgements

The authors wish to thank Dr Saeideh Ebrahimiasl for editing this manuscript for English language.

References

1 A. Mateska, G. Stojković, B. Mikhova, K. Mladenovska and E. Popovski, *ARKIVOC*, 2009, **10**, 131–140.

2 (*a*) N. Kambe, T. Iwasaki and J. Terao, *Chem. Soc. Rev.*, 2011, **40**, 4937–4947; (*b*) C. M. So and F. Y. Kwong, *Chem. Soc. Rev.*, 2011, **40**, 4963–4972; (*c*) Z. Shao and H. Zhang, *Chem. Soc. Rev.*, 2012, **41**, 560–572; (*d*) J. Xie, H. Jin and A. S. K. Hashmi, *Chem. Soc. Rev.*, 2017, **46**, 5193–5203.

3 A. d. Meijere and F. Diederich, *Metal-catalyzed cross-coupling reactions*. Weinheim, Wiley-VCH Verlag GmbH, 2004, vol. 1.

4 (*a*) C. S. Yeung and V. M. Dong, *Chem. Rev.*, 2011, **111**, 1215–1292; (*b*) S. A. Girard, T. Knauber and C. J. Li, *Angew. Chem., Int. Ed. Engl.*, 2014, **53**, 74–100; (*c*) H. Wang, X. Gao, Z. Lv, T. Abdelilah and A. Lei, *Chem. Rev.*, 2019, **119**, 6769–6787.

5 (*a*) A. Fihri, M. Bouhrara, B. Nekoueishahraki, J.-M. Basset and V. Polshettiwar, *Chem. Soc. Rev.*, 2011, **40**, 5181–5203; (*b*) K. Nejati, S. Ahmadi, M. Nikpassand, P. D. K. Nezhad and E. Vessally, *RSC Adv.*, 2018, **8**, 19125–19143; (*c*) A. Monfared, R. Mohammadi, S. Ahmadi, M. Nikpassand and A. Hosseinian, *RSC Adv.*, 2019, **9**, 3185–3202; (*d*) S. Mohammadi, M. Musavi, F. Abdollahzadeh, Babadoust and A. Hosseinian, *Chem. Rev. Lett.*, 2018, **1**, 49–55; (*e*) E. Najafi, F. Behmagham, N. Shaabani and N. Shojaei, *Chem. Rev. Lett.*, 2019, **2**, 13–20; (*f*) M. Chabanea and B. Dahmani, *Chem. Rev. Lett.*, 2019, **2**, 118–122.

6 (*a*) E. Vessally, M. Babazadeh, A. Hosseinian, S. Arshadi and L. Edjlali, *J. CO2 Util.*, 2017, **21**, 491–502; (*b*) K. Didehban, E. Vessally, A. Hosseinian, L. Edjlali and E. S. Khosroshahi, *RSC Adv.*, 2018, **8**, 291–301; (*c*) A. Hosseinian, S. Ahmadi, A. Monfared, P. D. Nezhad and E. Vessally, *Curr. Org. Chem.*, 2018, **22**, 1862–1874; (*d*) E. Vessally, K. Didehban, R. Mohammadi, A. Hosseinian and M. Babazadeh, *J. Sulfur Chem.*, 2018, **39**, 332–349; (*e*) S. Shahidi, P. Farajzadeh, P. Ojaghloo, A. Karbakhshzadeh and A. Hosseinian, *Chem. Rev. Lett.*, 2018, **1**, 37–44.

7 (*a*) A. Hosseinian, S. Farshbaf, L. Z. Fekri, M. Nikpassand and E. Vessally, *Top. Curr. Chem.*, 2018, **376**, 23; (*b*) F. A. H. Nasab, L. Z. Fekri, A. Monfared, A. Hosseinian and E. Vessally, *RSC Adv.*, 2018, **8**, 18456–18469; (*c*) A. Hosseinian, S. Ahmadi, F. A. H. Nasab, R. Mohammadi and E. Vessally, *Top. Curr. Chem.*, 2018, **376**, 39; (*d*) A. Hosseinian, F. A. H. Nasab, S. Ahmadi, Z. Rahmani and E. Vessally, *RSC Adv.*, 2018, **8**, 26383–26398; (*e*) A. Hosseinian, R. Mohammadi, S. Ahmadi, A. Monfared and Z. Rahmani, *RSC Adv.*, 2018, **8**, 33828–33844; (*f*) W. Peng, E. Vessally, S. Arshadi, A. Monfared, A. Hosseinian and L. Edjlali, *Top. Curr. Chem.*, 2019, **377**, 20; (*g*) A. Monfared, S. Ebrahimiasl, M. Babazadeh, S. Arshadi and E. Vessally, *J. Fluorine Chem.*, 2019, **220**, 24–34; (*h*) S. Arshadi, S. Ebrahimiasl, A. Hosseinian, A. Monfared and E. Vessally, *RSC Adv.*, 2019, **9**, 8964–8976; (*i*) M. Hamzeloo, A. Hosseinian, S. Ebrahimiasl, A. Monfared and E. Vessally, *J. Fluorine Chem.*, 2019, **224**, 52–60; (*j*) S. Arshadi, A. Banaei, A. Monfared, S. Ebrahimiasl and A. Hosseinian, *RSC Adv.*, 2019, **9**, 17101–17118; (*k*) A. Hosseinian, S. Arshadi, S. Sarhandi, A. Monfared and E. Vessally, *J. Sulfur Chem.*, 2019, **40**, 289–311; (*l*) A. Hosseinian, P. D. K. Nezhad, S. Ahmadi, Z. Rahmani and A. Monfared, *J. Sulfur Chem.*, 2019, **40**, 88–112; (*m*) S. Sarhandi, M. Daghagheleh, M. Vali, R. Moghadami and E. Vessally, *Chem. Rev. Lett.*, 2018, **1**, 9–15; (*n*) M. Daghagheleh, M. Vali, Z. Rahmani, S. Sarhandi and E. , *Chem. Rev. Lett.*, 2018, **1**, 23–30; (*o*)

S. Farshbaf, L. Sreerama, T. Khodayari and E. Vessally, *Chem. Rev. Lett.*, 2018, **1**, 56–67.
8 K. Li, Q. Wu, J. Lan and J. You, *Nat. Commun.*, 2015, **6**, 8404.
9 J. Xie and C. Zhu, *Sustainable C (sp^3)–H Bond Functionalization*, Springer, 2016.
10 T. Zeng, G. Song, A. Moores and C.-J. Li, *Synlett*, 2010, **2010**, 2002–2008.
11 M. Rueping, J. Zoller, D. C. Fabry, K. Poscharny, R. M. Koenigs, T. E. Weirich and J. Mayer, *Chem.–Eur. J.*, 2012, **18**, 3478–3481.
12 Q.-Y. Meng, Q. Liu, J.-J. Zhong, H.-H. Zhang, Z.-J. Li, B. Chen, C.-H. Tung and L.-Z. Wu, *Org. Lett.*, 2012, **14**, 5992–5995.
13 R. Hudson, S. Ishikawa, C.-J. Li and A. Moores, *Synlett*, 2013, **24**, 1637–1642.
14 H. E. Ho, Y. Ishikawa, N. Asao, Y. Yamamoto and T. Jin, *Chem. Commun.*, 2015, **51**, 12764–12767.
15 W. Yang, L. Wei, T. Yan and M. Cai, *Catal. Sci. Technol.*, 2017, **7**, 1744–1755.
16 S. Li, D. P. Shelar, C.-C. Hou, Q.-Q. Chen, P. Deng and Y. Chen, *J. Photochem. Photobiol., A*, 2018, **363**, 44–50.
17 W. Liang, T. Zhang, Y. Liu, Y. Huang, Z. Liu, Y. Liu, B. Yang, X. Zhou and J. Zhang, *ChemSusChem*, 2018, **11**, 3586–3590.
18 P. Li, G.-W. Wang, X. Zhu and L. Wang, *Tetrahedron*, 2019, **75**, 3448–3455.
19 P. Rana, R. Gaur, R. Gupta, G. Arora, J. Anireddy and R. K. Sharma, *Chem. Commun.*, 2019, **55**, 7402–7405.
20 J. Dong, W. Min, H. Li, Z. Quan, C. Yang and C. Huo, *Adv. Synth. Catal.*, 2017, **359**, 3940–3944.
21 I. Martín-García and F. Alonso, *Chem.–Eur. J.*, 2018, **24**, 18857–18862.
22 Q.-Y. Meng, J.-J. Zhong, Q. Liu, X.-W. Gao, H.-H. Zhang, T. Lei, Z.-J. Li, K. Feng, B. Chen, C.-H. Tung and L.-Z. Wu, *J. Am. Chem. Soc.*, 2013, **135**, 19052–19055.
23 M. Lin, L.-X. Dai, J. Gu, L.-Q. Kang, Y.-H. Wang, R. Si, Z.-Q. Zhao, W.-C. Liu, X. Fu, L.-D. Sun, Y.-W. Zhang and C.-H. Yan, *RSC Adv.*, 2017, **7**, 33078–33085.
24 A. Tyagi, A. Yamamoto and H. Yoshida, *RSC Adv.*, 2018, **8**, 24021–24028.
25 X. Marset, J. M. Pérez and D. J. Ramón, *Green Chem.*, 2016, **18**, 826–833.
26 F. Alonso, A. Arroyo, I. Martín-García and Y. Moglie, *Adv. Synth. Catal.*, 2015, **357**, 3549–3561.
27 S. Gupta, H. Joshi, N. Jain and A. K. Singh, *J. Mol. Catal. Chem.*, 2016, **423**, 135–142.
28 T. Dang-Bao, C. Pradel, I. Favier and M. Gómez, *Adv. Synth. Catal.*, 2017, **359**, 2832–2846.
29 (*a*) E. Vessally, *RSC Adv.*, 2016, **6**, 18619–18631; (*b*) E. Vessally, L. Edjlali, A. Hosseinian, A. Bekhradnia and M. D. Esrafili, *RSC Adv.*, 2016, **6**, 49730–49746; (*c*) E. Vessally, S. Soleimani-Amiri, A. Hosseinian, L. Edjlali and A. Bekhradnia, *RSC Adv.*, 2017, **7**, 7079–7091; (*d*) S. Arshadi, E. Vessally, L. Edjlali, R. Hosseinzadeh-Khanmiri and E. Ghorbani-Kalhor, *Beilstein J. Org. Chem.*, 2017, **13**, 625–638; (*e*) S. Arshadi, E. Vessally, M. Sobati, A. Hosseinian and A. Bekhradnia, *J. CO2 Util.*, 2017, **19**, 120–129.
30 J.-A. García-López and M. F. Greaney, *Chem. Soc. Rev.*, 2016, **45**, 6766–6798.
31 D. A. Horton, G. T. Bourne and M. L. Smythe, *Chem. Rev.*, 2003, **103**, 893–930.
32 P. E. Fanta, *Synthesis*, 1974, 9–21.
33 F.-X. Felpin and S. Sengupta, *Chem. Soc. Rev.*, 2019, **48**, 1150–1193.
34 J. Wencel-Delord, A. Panossian, F. Leroux and F. Colobert, *Chem. Soc. Rev.*, 2015, **44**, 3418–3430.
35 I. Hussain and T. Singh, *Adv. Synth. Catal.*, 2014, **356**, 1661–1696.
36 L. M. Neal and H. E. Hagelin-Weaver, *J. Mol. Catal. Chem.*, 2008, **284**, 141–148.
37 T. Ishida, R. Tsunoda, Z. Zhang, A. Hamasaki, T. Honma, H. Ohashi, T. Yokoyama and M. Tokunaga, *Appl. Catal., B*, 2014, **150**, 523–531.
38 P. Serna and A. Corma, *J. Catal.*, 2014, **315**, 41–47.
39 P. Serna and A. Corma, *ChemSusChem*, 2014, **7**, 2136–2139.
40 T. Ishida, S. Aikawa, Y. Mise, R. Akebi, A. Hamasaki, T. Honma, H. Ohashi, T. Tsuji, Y. Yamamoto and M. Miyasaka, *ChemSusChem*, 2015, **8**, 695–701.
41 S. Tabasso, E. C. Gaudino, E. Acciardo, M. Manzoli, A. Giacomino and G. Cravotto, *Molecules*, 2019, **24**, 288.
42 S. I. Kozhushkov and L. Ackermann, *Chem. Sci.*, 2013, **4**, 886–896.
43 (*a*) X. Shang and Z.-Q. Liu, *Chem. Soc. Rev.*, 2013, **42**, 3253–3260; (*b*) C. Aouf, E. Thiery, J. Le Bras and J. Muzart, *Org. Lett.*, 2009, **11**, 4096–4099; (*c*) Z. Shi, N. Schröder and F. Glorius, *Angew. Chem., Int. Ed. Engl.*, 2012, **51**, 8092–8096; (*d*) G. G. Pawar, G. Singh, V. K. Tiwari and M. Kapur, *Adv. Synth. Catal.*, 2013, **355**, 2185–2190; (*e*) S. Maity, R. Kancherla, U. Dhawa, E. Hoque, S. Pimparkar and D. Maiti, *ACS Catal.*, 2016, **6**, 5493–5499.
44 L. L. Chng, J. Zhang, J. Yang, M. Amoura and J. Y. Ying, *Adv. Synth. Catal.*, 2011, **353**, 2988–2998.
45 Q. Hu, X. Liu, G. Wang, F. Wang, Q. Li and W. Zhang, *Chem. Eur. J.*, 2017, **23**, 17659–17662.
46 (*a*) J.-J. Brunet and R. Chauvin, *Chem. Soc. Rev.*, 1995, **24**, 89–95; (*b*) F. Boscá and M. A. Miranda, *J. Photochem. Photobiol., B*, 1998, **43**, 1–26; (*c*) J. Panten and K. Bauer, *Common Fragrance and Flavor Materials: Preparation, Properties and Uses*, Wiley VCH, 2006.
47 X. F. Wu, *Chem. Eur. J.*, 2015, **21**, 12252–12265.
48 T. Ramani, P. Umadevi, K. L. Prasanth and B. Sreedhar, *Eur. J. Org. Chem.*, 2013, 6021–6026.
49 C. A. Menendez, F. Nador, G. Radivoy and D. C. Gerbino, *Org. Lett.*, 2014, **16**, 2846–2849.
50 Q. Hu, X. Liu, F. Huang, F. Wang, Q. Li and W. Zhang, *Catal. Commun.*, 2018, **113**, 27–31.
51 S. Kaur, M. Kumar and V. Bhalla, *Green Chem.*, 2016, **18**, 5870–5883.
52 (*a*) M. Villegas, D. Vargas, J. Msonthi, A. Marston and K. Hostettmann, *Planta Med.*, 1988, **54**, 36–37; (*b*) E.-A. Bae, M. J. Han, N.-I. Baek and D.-H. Kim, *Arch. Pharmacal Res.*, 2001, **24**, 297–299; (*c*) S. Purup, E. Larsen and L. P. Christensen, *J. Agric. Food Chem.*, 2009, **57**, 8290–8296; (*d*) H. Kim, J. Chin, H. Choi, K. Baek, T.-G. Lee,

S. E. Park, W. Wang, D. Hahn, I. Yang and J. Lee, *Org. Lett.*, 2013, **15**, 100–103.
53 W. Shi and A. Lei, *Tetrahedron Lett.*, 2014, **55**, 2763–2772.
54 (*a*) C. Glaser, *Chem. Ber.*, 1869, **2**, 422–424; (*b*) J. Tang, H. Jiang, G. Deng and L. Zhou, *Chin. J. Org. Chem.*, 2005, **25**, 1503–1507; (*c*) Z. M. Nimmo, J. F. Halonski, L. E. Chatkewitz and D. D. Young, *Bioorg. Chem.*, 2018, **76**, 326–331.
55 F. Nador, L. Fortunato, Y. Moglie, C. Vitale and G. Radivoy, *Synthesis*, 2009, 4027–4031.
56 B. X. Tang, X. N. Fang, R. Y. Kuang, J. H. Wu, Q. Chen, S. J. Hu and Y. L. Liu, *Appl. Organomet. Chem.*, 2016, **30**, 943–945.
57 F. Alonso, T. Melkonian, Y. Moglie and M. Yus, *Eur. J. Org. Chem.*, 2011, 2524–2530.
58 S. Biswas, K. Mullick, S.-Y. Chen, D. A. Kriz, M. Shakil, C.-H. Kuo, A. M. Angeles-Boza, A. R. Rossi and S. L. Suib, *ACS Catal.*, 2016, **6**, 5069–5080.
59 X. Zhao, X. Lu, A. Wei, X. Jia, J. Chen and K. Lu, *Tetrahedron Lett.*, 2016, **57**, 5330–5333.
60 B. Maaten, J. Moussa, C. Desmarets, P. Gredin, P. Beaunier, T. Kanger, K. Tõnsuaadu, D. Villemin and M. Gruselle, *J. Mol. Catal. Chem.*, 2014, **393**, 112–116.
61 W. Lu, W. Sun, X. Tan, L. Gao and G. Zheng, *Catal. Commun.*, 2019, **125**, 98–102.
62 H. Li, M. Yang and Q. Pu, *Microporous Mesoporous Mater.*, 2012, **148**, 166–173.
63 X. Li, D. Li, Y. Bai, C. Zhang, H. Chang, W. Gao and W. Wei, *Tetrahedron*, 2016, **72**, 6996–7002.
64 M. Boronat, S. Laursen, A. Leyva-Pérez, J. Oliver-Meseguer, D. Combita and A. Corma, *J. Catal.*, 2014, **315**, 6–14.
65 C. Gonzalez-Arellano, A. M. Balu, R. Luque and D. J. Macquarrie, *Green Chem.*, 2010, **12**, 1995–2002.
66 S. B. Patel and D. V. Vasava, *ChemistrySelect*, 2018, **3**, 471–480.
67 F. Nador, M. A. Volpe, F. Alonso, A. Feldhoff, A. Kirschning and G. Radivoy, *Appl. Catal., A*, 2013, **455**, 39–45.
68 J. M. Perez, R. Cano, M. Yus and D. J. Ramon, *Synthesis*, 2013, **45**, 1373–1379.
69 F. Farzaneh, Z. Shafie, E. Rashtizadeh and M. Ghandi, *React. Kinet., Mech. Catal.*, 2013, **110**, 119–129.
70 Z. Chen, R. Shen, C. Chen, J. Li and Y. Li, *Chem. Commun.*, 2018, **54**, 13155–13158.
71 H. Peng, Y. Xi, N. Ronaghi, B. Dong, N. G. Akhmedov and X. Shi, *J. Am. Chem. Soc.*, 2014, **136**, 13174–13177.
72 L. Liu, T. Matsushita, P. Concepción, A. Leyva-Pérez and A. Corma, *ACS Catal.*, 2016, **6**, 2211–2221.
73 B. t. Vilhanová, J. i. Václavík, L. Artiglia, M. Ranocchiari, A. Togni and J. A. van Bokhoven, *ACS Catal.*, 2017, **7**, 3414–3418.
74 C. T. Ma, J. J. Wang, A. D. Zhao, Q. L. Wang and Z. H. Zhang, *Appl. Organomet. Chem.*, 2017, **31**, e3888.
75 D. Chakraborty, S. Nandi, D. Mullangi, S. Haldar, C. P. Vinod and R. Vaidhyanathan, *ACS Appl. Mater. Interfaces*, 2019, **11**, 15670–15679.